Design, fabrication, characterization and

in vitro **digestion of alkaloid-, catechin-, and cocoa extract-loaded liposomes**

Said Toro-Uribe[a], Elena Ibáñez[b], Eric A. Decker[c], David Julian McClements[d], Ruojie Zhang[d], Luis Javier López-Giraldo[a], Miguel Herrero[b*],

[a]Food Science & Technology Research Center (CICTA), School of Chemical Engineering, Universidad Industrial de Santander, Carrera 27, Calle 9, 68002 - Bucaramanga, Colombia.

[b]Foodomics Laboratory, Institute of Food Science Research (CIAL, CSIC-UAM), Nicolás Cabrera 9, 28049 - Madrid, Spain.

[c]Chenoweth Laboratory, Department of Food Science, University of Massachusetts, 100 Holdsworth Way, Amherst, MA 01003, USA

[d]Biopolymers & Colloids Research Laboratory, Department of Food Science, University of Massachusetts, 100 Holdsworth Way, Amherst, MA 01003, USA

*Corresponding author: Tel: +34 910 017 946; FAX: +34 910 017 905; E-mail: m.herrero@csic.es.

ABSTRACT

Liposomes containing theobromine, caffeine, catechin, epicatechin, and a cocoa extract were fabricated using microfluidization and sonication. A high encapsulation efficiency and good physicochemical stability were obtained by sonication (75% amplitude, 7 min). Liposomes produced at pH 5.0 had mean particle diameter ranging from 73.9 to 84.3 nm. The structural and physicochemical properties of the liposomes were characterized by transmission electron microscopy, confocal fluorescence microscopy and antioxidant activity assays. The release profile was measured by Ultra-High Performance Liquid Chromatography coupled to diode array detection. The bioaccessibility of the bioactive compounds encapsulated in liposomes was determined after exposure to a simulated *in vitro* digestion model. Higher bioaccessibilities were measured for all catechins-loaded liposome formulations compared to non-encapsulated counterparts. These results demonstrated that liposomes are capable of increasing the bioaccessibility of flavan-3-ols, which may be important for the development of nutraceutical-enriched functional foods.

Keywords: Alkaloids, Catechins, Cocoa polyphenols, Liposomes, *In vitro* digestion.

INTRODUCTION

Polyphenols are secondary metabolites found in plants that are considered to be the most abundant phytochemicals in our diet.[1] The main dietary sources of polyphenols are fruits, beverages, vegetables, whole grains, and cereals.[1] In particular, coffee-, tea-, grape-, apple-, and cocoa-based products have become one of the most important and popularly consumed food and beverage sources of polyphenols globally. Catechins and alkaloids are the most notable secondary metabolites found in these sources with an average daily intake of 84 mg for caffeine and 17 - 39 mg for flavan-3-ols for a body weight of 70 kg.[2,3] Catechins (such as (-)-epicatechin and (+)-catechin) and alkaloids (such as theobromine and caffeine) are also the major secondary metabolites in cocoa constituting up to 35 wt.% of the total phenolics and 3 wt.% on a fat-free basis, respectively.[4] Alkaloids stimulate the nervous system and act as vasodilators, and are toxic to many animals.[5] Catechins are chemically characterized by possessing several hydroxyl groups in their structure, and have been shown to exhibit several health benefits, which have been discussed in detail by Cirillo[6] and Kumar & Pandey.[7]

Despite their good antioxidant activities, several reports have highlighted that catechins are unstable during storage and processing, and are sensitive to oxidation, light, and pH.[8] Poor stability under gastrointestinal conditions has also been reported for several groups of polyphenols. For instance, the plasma concentration of phenolic acids, monomeric flavanols, procyanidins B1 and B2, and quercetin rarely exceeds 1 μM.[9] Ovando et al.[10] reported that total flavonoids and polyphenols decreased by 83% and 77%, and 87 and 97% in gastric and intestinal phases, respectively. Moreover, the DPPH radical scavenging activity was reduced by 62% within the gastric phase, while it increased by 27% within the intestinal phase.

The oral bioavailability of polyphenols depends on a variety of factors, including the release from the food matrix during gastrointestinal digestion, solubilization in the intestinal fluids, transport across the mucus layer, cellular uptake, metabolism, and further transport in the circulatory system.[9] Bioaccessibility is defined as the fraction of polyphenols released from the food matrix that are in a form that is suitable for intestinal absorption. Thus, the overall bioactivity of polyphenols depends on the amount present in the original plant, as well as the fraction that can actually be absorbed.[10] For example, Lee[11] reported that when epigallocatechin gallate was administered, only 0.1% of the ingested dose appeared in the blood and the fraction absorbed is preferentially excreted through the bile to the colon. Meanwhile, epigallocatechin and epicatechin appear to be more bioavailable, but the fractions of these compounds that appeared in the plasma are also low, and only 3.3 and 8.9% of the ingested substances were excreted in the urine.

Encapsulating bioactive compounds into well-designed colloidal delivery systems could help to overcome some of the above limitations. Previous studies have investigated the factors that affect the bioaccessibility and bioavailability of commercial flavonoids and/or polyphenolic extracts from several plant sources (e.g., cocoa, tea, apple, pepper, and carrots) using *in vitro* or *in vivo* studies.[9–13] In the case of cocoa polyphenols, several studies have been carried out, based on microencapsulation in a carbohydrate matrix by spray drying (e.g., starches and maltodextrins),[14] on electrostatic extrusion in alginate-chitosan microbeads,[15] and on encapsulation through emulsion electrospraying.[16] However, many of these technologies produced large particle sizes, irregular particle shapes, and do not allow the incorporation of polyphenols with different polarities,[8] for example, with different degrees of galloylation or polymerization.[17]

A variety of colloidal delivery systems have also been assessed for their potential to encapsulate these types of nutraceuticals, including: nanoemulsions,[18] W/O/W emulsion,[19] and uncoated[17] or coated liposomes (e.g., with chitosan, calcium pectinate, or hydroxypropyl methylcellulose).[20,21]

63 Liposome-based systems are considered to be particularly suitable for encapsulation and delivery
64 for both water- and oil-soluble functional compounds.[20] Liposomes are typically spherical, single-
65 or multi-layered vesicles, having an aqueous core enclosed by one or more membrane-like
66 concentric bilayers with diameters ranging from tens of nanometers to several micrometers.[22,23] Due
67 to their ability to encapsulate both hydrophilic and hydrophobic bioactives, liposomes have gained
68 attention in the food and pharmaceutical industries as promising delivery systems for polyphenolic
69 compounds. In particular, they can be designed to increase the dispersibility, to protect from
70 degradation, and to increase the bioavailability of polyphenols. In general, the bioavailability of
71 encapsulated components is higher in nanoliposomes (d = 10 to 100 nm) than in conventional
72 liposomes (d > 100 nm). However, preparation of nanoliposome-based delivery systems is
73 challenging using traditional methods because of difficulties in generating small particle sizes and
74 ensuring high entrapment efficiency.[24]

75 Several factors impact the physicochemical performance of liposomes, including the nature of
76 the phospholipids used to fabricate them. For example, soybean lecithin contains high amounts of
77 C18:2 and C18:3, and is susceptible to hydrolysis of the ester bonds and peroxidation of the
78 unsaturated acyl chains,[22] producing off-flavors and oxidation of the bioactive encapsulated within
79 the liposomes.[17] Moreover, the preparation method can affect the shelf-life of liposomes (*e.g.,* due
80 to leakage, aggregation, or separation), and impacts their encapsulation efficiency, thereby, affecting
81 their efficacy as delivery systems.

82 The aim of this study was to develop a suitable food-grade method for liposome preparation
83 using soybean lecithin, and to compare the bioaccessibility of catechins, alkaloids and whole cocoa
84 extract under simulated gastrointestinal fluids. The process parameters were optimized to achieve a
85 small particle size, narrow polydispersity, extended shelf life, and high encapsulation efficiency.

The effect of sonication and microfluidization parameters on the formation and performance of the delivery systems was also evaluated so as to identify optimized conditions to produce them.

MATERIALS AND METHODS

Reagents and Samples

All chemicals used were of analytical grade and used with no further purification. L-α-phosphatidylcholine from soybean (Type IV-S ≥ 30% PC), (+)-catechin hydrate, 2,2-diphenyl-1-picrylhydrazyl (DPPH), 2,2'-azino-bis (3-ethylbenzothiazoline-6-sulfonic acid) diammonium salt (ABTS), trolox ((±)-6-hydroxy-2,5,7,8-tetramethylchromane-2-carboxylic acid), hexanal, Nile red (72485), Triton X-100, cumene hydroperoxide, iron (II) sulfate heptahydrate, barium chloride dehydrate, ammonium thiocyanate, potassium persulfate, potassium chloride, potassium dihydrogen phosphate, sodium bicarbonate, magnesium chloride hexahydrate, ammonium carbonate, calcium chloride, α-amylase (type IX-A), porcine pepsin, porcine pancreatic lipase, and bile salts were obtained from Sigma Aldrich (Sigma–Aldrich, Steinheim, Germany). (–)-Epicatechin (purity ≥ 99%) was purchased from ChromaDex Inc. (Irvine, CA, USA). Sodium acetate trihydrate, hydrochloric acid, glacial acetic acid, ethanol, methanol, and 1-butanol were obtained from Fisher Scientific (Fair Lawn, NJ, USA). Decanox MTS-90G mixed with tocopherols were obtained by ADM (Archer Daniels Midland Company, Decatur, IL, USA). Milli-Q water (Millipore system, Billerica, MA, USA) and deionized water were used for the preparation of all solutions. To minimize the presence of metals contaminants, all the glassware was acid-washed.

Polyphenolic extract recovered from unfermented cocoa beans with low polyphenol oxidase activity was obtained according to our previous published procedure.[17,25] Briefly, cocoa beans (variety ICS-39) were separated manually from the cocoa husk and the mucilage coating around each bean was removed. After that, polyphenol oxidase were inactivated by placing the cocoa beans in a 70 mM

ascorbic acid/L-cysteine (1:1 v/v) solution and thermally processed at 96 ºC for 6.4 min. Beans with reduced enzymatic activity were chopped and oven-dried at 70 ºC for 3h. Dried beans were milled at cryogenic conditions (Retsch Technology GmbH, Haan, Germany) to particle sizes lower than 0.18 mm. Recovery of polyphenols was carried out by ultrasound-assisted solid-liquid extraction using 50% ethanol at 20 kHz for 30 min (Elma, Ultrasonic LC 30H, Germany) followed by incubation at 70 ºC for 45 min under constant stirring. The resulting extract was centrifuged (Heraeus, Megafuge 16R, Thermo Scientific, Germany), concentrated by vacuum evaporation (R-100, Büchi, Switzerland) and then freeze-dried (Model 18, Labconco Corp., Kansas City, MO, USA). The resulting violet-powder was stored at -80 ºC until further analysis.

Liposome preparation

Soy lecithin was added to sodium acetate-acetic acid buffer (0.1 M; pH 3.0 ± 0.1 or pH 5.0 ± 0.1) containing 2.5% (v/v) ethanol, and final lecithin concentrations of 1, 3, 5, or 10% (w/v). Pre-homogenization was carried out by stirring the system at 25 ºC until complete dissolution, followed by homogenization with a high shear blender (T10 Ultra-Turrax, IKA, Staufen, Germany) at 20,000 rpm for 2 min. The resulting coarse liposome suspension was then further homogenized using two different approaches: (1) *microfluidization* (110T, Microfluidics, Newton, MA, USA) at 137.9 MPa (20000 psi) for several passages (up to 8 cycles) in an ice bath (4 ºC); or (2) *sonication* (Model 505, Fisher Scientific, USA) with a sonicator probe set at 10 s on/off pulses and submerged 1 cm from the bottom of a container placed in an ice water around 4 ºC. The amplitude (50 to 75%) and time of sonication (2.5 to 15 min) were varied. The liposomal solutions prepared were then filtered through 0.45 µm hydrophilic PTFE filter (Millipore, Milford, MA, USA).

Bioactive compounds (1000 µM) were dissolved in ethanol (2.5% v/v) and then added to a 0.1 M sodium acetate-acetic acid buffer solution (pH 3.0 ± 0.1 or pH 5.0 ± 0.1). Soy lecithin was then added and the mixture was homogenized as described above. Liposomes without active ingredient

133 (control) were also prepared. The bioactive compounds tested were (+)-catechin (C), (-)-epicatechin
134 (EC), theobromine (Theo), caffeine (Caf), and cocoa extract.

135 **Characterization of liposomes**

136 *Particle size and ζ-potential measurements*

137 The mean particle diameter, polydispersity index (PDI), and ζ-potential were measured using a
138 combined dynamic light scattering/electrophoresis instrument (Nano-ZS, Malvern Instruments,
139 Worcestershire, UK) according to Panya et al.[23] The particle size distribution was calculated using
140 the Stokes-Einstein equation while the ζ-potential was calculated using the Smoluchowski model.
141 Liposome suspensions were diluted with an appropriate buffer (sodium acetate-acetic acid buffer
142 solution; 0.1M; pH 3.0 ± 0.1 or pH 5.0 ± 0.1) prior to analysis to prevent multiple scattering effects.

143 *Encapsulation efficiency*

144 The level of bioactive encapsulated within the liposomes was determined by measuring the
145 amount of free bioactive in the aqueous phase of a liposome suspension according to the method of
146 Toro-Uribe et al.[17] with few modifications. Briefly, the samples were transferred to Optiseal bell-
147 top ultracentrifuge tubes (Beckman Coulter, USA) and high-speed centrifuged (Beckman L-70, 70
148 Ti rotor, Beckman Instruments Inc, CA, USA) at 50,000 rpm, 4 ºC for 2 h. Then, the supernatant
149 (200 µL) was carefully collected and used to determine bioactive concentrations using analytical
150 reverse phase UHPLC-DAD as described later. Encapsulation efficiency (EE) was expressed on a
151 weight percentage basis according to the following equation:

152 $$EE(\%) = \frac{C_i - C_{free}}{C_i} * 100$$

153 C_i is the initial concentration of bioactive added to the liposomes and C_{free} is the concentration of
154 free bioactive remaining in the aqueous phase.

155 **Physicochemical stability**

156 *Influence of pH*

157 As liposomes are pH-sensitive, the impact of both pH 3.0 ± 0.1 and pH 5.0 ± 0.1 on the oxidative
158 stability (lipid hydroperoxide and hexanal formation) and encapsulation efficiency of the liposomes
159 was determined. To do so, unloaded and 125 µM of EC-loaded liposomes (5 wt.%) were incubated
160 at 55 °C. Based on these results, pH 5.0 ± 0.1 was chosen and used for further studies.

161 *Influence of temperature and storage time*

162 The impact of temperature on the storage stability of the liposomes was determined by placing
163 the liposome suspension (1 mL, pH = 5.0) into 10 mL headspace vials, that were then sealed with
164 poly(tetrafluoroethylene) butyl septa, and incubated at 4, 32, 37, and 55 °C in the dark. Samples
165 were collected at several time points (0 to 20, 30, 35, 40, 45, 50, 60, 90, 120, 150, 180, 210, 240,
166 270, 300 days) and immediately analyzed. The changes in particle size and ζ-potential were
167 determined as previously mentioned, and color and hexanal formation were also measured as
168 described later.

169 Lipid oxidation was analyzed by monitoring lipid hydroperoxides (a primary oxidation product)
170 and headspace hexanal (a secondary oxidation product) at various time points. Hydroperoxides were
171 analyzed according to the spectrophotometric method described by Hu et al.[26] Samples (300 µL)
172 were mixed with 2.8 mL of methanol/butanol (2:1 v/v), then 15 µL of 3.94 M ammonium
173 thiocyanate and 15 µL of 0.072 M Fe^{2+} (ferrous sulfate) were added. The ferrous sulfate solution
174 was made by mixing 0.13 M $BaCl_2$ and 0.14 M $FeSO_4$. The reaction was incubated in the dark at
175 room temperature for 20 min, and the absorbance was measured at 510 nm (Genesys 20, Thermo
176 Scientific, Waltham, MA, USA). The calculation was made from a standard curve of cumene
177 hydroperoxide (0 – 0.6 mM, $r^2 = 0.99$) and data is expressed as mmol hydroperoxide per kg lecithin.

178 Gas chromatography (GC) was utilized to quantify headspace hexanal. A GC instrument
179 equipped with a headspace autosampler and flame ionization detector (FID) (Shimadzu GC 2014,
180 Shimadzu, Tokyo, Japan) was used. The operating parameters used were selected according to Hu
181 et al.[26] Briefly, samples were incubated for 10 min at 55 ºC in their sealed containers. A 50/30 µm
182 DVB/Carboxen/PDMS solid-phase microextraction (SPME, Supelco, Bellefonte, PA, USA) fiber
183 needle pierced the silicone/PTFE septa to a depth of 22 mm and adsorbed volatiles for 6 min. Then,
184 the fiber was placed in the injector (250 ºC) port at a split ratio of 1:7 and desorbed for 3 min. The
185 GC separation was isothermal at 65 ºC for 10 min on a HP methyl silicone (DB-1) fused-silica
186 capillary column (50 m, 0.31 mm diameter x 1 µm) (Supelco, Bellefonte, PA, USA). Other
187 parameters include pressurization 10 s; venting 10 s and helium as a carrier gas. A standard curve
188 using hexanal (0 – 50 mM) was prepared to calculate hexanal concentrations in the samples (r^2 =
189 0.99). Data are expressed as mmol hexanal kg^{-1} lecithin.

190 Based on both peroxide value and hexanal formation *versus* storage time plots, the lag phase
191 was determined to quantify the time for lipid oxidation. The lag phase was defined as the last day
192 before there was a statistically significant increase in the concentration of primary or secondary
193 oxidation products before the exponential phase was entered.

194 *Color measurement*

195 The color of the liposomes was measured using an instrumental colorimeter (ColorFlex,
196 HunterLab Reston, VA, USA) to evaluate changes in the appearance of the liposome suspensions
197 due to lipid peroxidation as previously described.[27] To do so, 10 mL of liposome suspensions were
198 collected at different time points and placed into a Petri dish to perform the analysis. The total color
199 difference (ΔE) was calculated from the CIE tristimulus color coordinates as follows:

200 $$\Delta E = \sqrt{(L^* - L_i^*)^2 + (a^* - a_i^*)^2 + (b^* - b_i^*)^2}$$

L*a*b* values are the CIE tristimulus color coordinates: *L** (black to white) represents the lightness; *a** represents red to green; and *b** represents yellow to blue. The subscript *i* represents the initial color values. Additionally, the color intensity of the samples was calculated through the difference in the chroma (ΔC*) values:

$$\Delta C^* = \sqrt{(a^* - a_i^*)^2 + (b^* - b_i^*)^2}$$

In vitro digestion stability of liposomes

Simulated digestion model

Three groups of samples were studied (i) bioactive-loaded liposomes; (ii) empty liposomes; (iii) bioactive compounds dispersed in aqueous solutions. The bioactive compounds consisted of (+)-catechin, (-)-epicatechin, theobromine, caffeine, and crude cocoa extract. The empty liposomes and aqueous systems were used as controls. All the samples were passed through a three-stage *in vitro* digestion model consisting of mouth, stomach, and small intestinal phases according to the standardized static method of Minekus et al.[28] as follows:

A simulated saliva fluid (SSF) consisting of 1.25-fold concentrated stock solution was prepared containing 15.1 mM KCl, 3.7 mM KH_2PO_4, 13.6 mM $NaHCO_3$, 0.15 mM $MgCl_2(H_2O)_6$, 0.06 mM $(NH_4)_2CO_3$, and 1.1 mM HCl. To carry out the assay, 25 mL of sample were mixed with 17.5 mL of SSF electrolyte solution, and then, 2.5 mL of 1500 U/mL salivary α-amylase solution in electrolyte stock solution were added, followed by 125 µL of 0.3 M $CaCl_2$, adjusted to pH 7 with 1 M HCl. Finally, the volume was made up to 50 mL with ultrapure water and the sample was incubated for 2 min at 37 ºC.

A simulated gastric fluid (SGF) electrolyte stock solution was prepared (1.25-fold concentrated) that consisted of 6.9 mM KCl, 0.9 mM KH_2PO_4, 25mM $NaHCO_3$, 47.2 mM NaCl, 0.1 mM

224 $MgCl_2(H_2O)_6$, 0.5 mM $(NH_4)_2CO_3$, and 15.6 HCl mM. After the oral phase, the sample was exposed
225 to the simulated gastric phase. To do that, 5 parts of liquid sample were mixed with 4 parts of SGF
226 stock electrolyte solution, and then, 4 mL of *ca.* 25000 U/mL porcine pepsin stock solution and 12.5
227 µL of 0.3 M $CaCl_2$ were added, followed by adjustment of the pH to 3 using 1 M HCl. Finally, the
228 volume was made up to 50 mL with deionized water and flushed with liquid nitrogen. The gastric
229 phase was carried out in a rotary shaker (Infors HT Multitron Standard, Switzerland) set at 100 rpm,
230 for 2 h at 37 ºC.

231 For the simulated *in vitro* dueodenal digestion, simulated intestinal fluid (SIF) was prepared
232 (1.25-fold concentrated) consisting of 6.8 mM KCl, 0.8 mM KH_2PO_4, 85mM $NaHCO_3$, 38.4 mM
233 NaCl, 0.33 mM $MgCl_2(H_2O)_6$, and 8.4 HCl mM. Then, 25 mL of gastric digest was mixed with
234 13.75 mL of SIF stock solution, 6.25 mL of 800 U/mL pancreatin, 3.125 mL of 160 mM fresh bile,
235 and 50 µL of 0.3 M $CaCl_2$. Then, the pH was adjusted to 7.0 with 1 M NaOH, and finally, the volume
236 was made up to 50 mL with deionized water and flushed with liquid nitrogen. The small intestine
237 phase was carried out in a rotary shaker (Infors HT Multitron Standard, Switzerland) set at 100 rpm,
238 for 6 h at 37 ºC.

239 *Release kinetics of bioactive compounds*

240 At predetermined time points (every 30 min during simulated gastric digestion, and every 1 h
241 during duodenal simulated digestion), 200 µL of dissolution media was withdrawn from each
242 digestion phase, and immediately snap frozen in liquid nitrogen and subsequently stored at -86 °C
243 (ULT Ultralow freezer, Haier, Quingdao, China) until further analysis. For quantitative analysis, the
244 samples were diluted and adjusted to pH 5. Then, the sample solution was centrifuged at 13400 rpm
245 for 30 min at 4 °C. The supernatant was carefully collected, considered as the total amount of
246 compound remaining (liposome-containing and free compound), and analyzed by UHPLC-DAD as
247 described later. The *in vitro* release behaviors were plotted as a function of time as follows:

$$Remaining\ (\%) = \frac{C_t}{C_i} * 100$$

where C_t is the sample concentration for each time point, and C_i is the initial concentration.

Determination of the bioaccessibility of the bioactive compounds

After *in vitro* digestion, 200 µL of raw digest was taken out and used for further analysis. To completely fracture the liposome membranes, samples were snap frozen in liquid nitrogen and conditioned at room temperature (repeated 5 times). Then, the sample was diluted with a solution containing 1% Triton X-100 and adjusted to pH 5. Subsequently, the sample was centrifuged (Heraeus Fresco 21, Thermo Scientific, Hamburg, Germany) at 13400 rpm, 4 ºC, for 30 min. The supernatant was carefully collected and considered to be the "micelle" fraction, in which the bioactive compounds were solubilized.[12] The amount of the bioactive present was quantified by UHPLC-DAD (see below), and the bioaccessibility was calculated as follows:

$$Bioaccessibility\ (\%) = \frac{C_{Digesta}}{C_i} * 100$$

where $C_{Digesta}$ and C_i are the concentrations of the bioactive compounds in the mixed micelle phase and the initial concentration, respectively.

Chromatographic analysis

The UHPLC system (Agilent 1290 Infinity series II, Agilent Tech. Santa Clara, CA, USA) consisted of a binary pump delivery system, an on-line degasser, a thermostated autosampler, and a diode array detector (DAD). System control and data analysis were processed using OpenLab CDS software (Agilent ChemStation). Diluted samples were filtered through a 0.45 µm hydrophilic Durapore PVDF membrane (Millipore, USA) and then 12 µL were injected into a C18 reverse phase Zorbax Eclipse Plus column (50 × 2.1 mm, 1.8 µm) connected to a Zorbax SB-C8 guard column (5 × 2.1 mm, 1.8 µm). The column oven was set at 55 ºC. The flow rate was 0.7 mL min^{-1} using water (0.01% formic acid, solvent A) and acetonitrile (0.01% formic acid, solvent B) as mobile phases. A

linear gradient program was performed as follows: 0 min, 0% B; 3.9 min, 1.5% B; 4.0 min, 4% B; 11.0 min, 10 %B; 14.0 min, 35% B; 14.2 min, 100% B; 16.5 min, 100% B; 17.0 min, 0% B; 23 min, 0% B. The resulting separation was recorded at 280 nm. All the samples were injected in triplicate. Additionally, a blank sample was injected between every sample. The content of (+)-catechin (0.05 – 100 ppm) , (-)-epicatechin (0.05 – 100 ppm), theobromine (0.05 – 25 ppm), and caffeine (0.1 – 50 ppm) in the tested samples were calculated from standard curves for each compound ($r^2 \geq 0.99$).

Microstructure and morphology analysis

Before and after *in vitro* digestion, 150 µL of either catechin-, epicatechin-, theobromine-, caffeine-, and cocoa extract-loaded liposome samples were taken for analysis using confocal optical scanning laser microscopy and transmission electron microscopy (TEM). Prior to analysis, samples were mixed with Nile Red solution (1 mg/mL) at a ratio 2/1 v/v, to dye the oil phase. Then, the dyed samples were placed on a microscope slide, covered by a coverslip, and observed by confocal optical scanning laser microscopy with a 60x oil immersion objective lens (Nikon D-Eclipse C1 80i, Nikon, Melville, NY, USA). The excitation and emission spectrum were set at 534/605 nm, respectively. The images were acquired using image analysis software (NIS-Elements, Nikon, Melville, NY).

TEM images were used to examine the morphology and to confirm the mean particle size of the samples. A liposome suspension (ca. 50 µL) was absorbed onto a Formvar carbon-coated 200 mesh thick grid (Ted Pella Inc., USA) for fixation for 2 min. Then, the grid was stained with uranyl acetate aqueous solution (2%) for 1 min and air-dried at room temperature, and the excess of liquid was removed with filter paper. The grid-sample was examined using a transmission electron microscope (JEOL JEM 1010, Tokyo, Japan) operating at an acceleration voltage of 100 keV, equipped with a Gatan ES1000W digital camera. The images were processed using Digital Micrograph software.

294 *Antioxidant assays*

295 The antioxidant activity of samples before and after the *in vitro* simulated digestion phases was
296 measured using two *in vitro* assays: DPPH$^{\bullet}$ and ABTS$^{\bullet+}$ free radicals scavenging assays. The DPPH
297 assay was carried according to the procedure described by Brand-Willians et al.[29] with the following
298 modifications: 68.5 µM of DPPH methanolic solution was diluted with methanol to obtain an
299 absorbance of 0.57 ± 0.01 units at 517 nm using a microplate reader (Synergy HT, BioTek
300 Instruments, Winooski, VT, USA) controlled by Gen5 software (Gen5 v. 2.04 BioTek Inst. Inc).
301 Then, 100 µL of sample was added to 745 µL of a methanolic solution of daily-working DPPH
302 solution at room temperature for 1 h in the dark. Lastly, 300 µL were taken out and placed in 96-
303 well microplates to measure their total absorbance. Methanol and DPPH• solution without test
304 samples were used as blank solutions and controls, respectively. Results are expressed as % radical
305 scavenging:

306 $$DPPH\ (\%) = \frac{Abs_{control} - Abs_{sample}}{Abs_{control}} * 100$$

307 For the ABTS assay, the antioxidant activity was assessed by their ability to scavenge the ABTS$^{\bullet+}$
308 free-radical cation using the method proposed by Re et al.[30] Briefly, ABTS$^{\bullet+}$ was produced by
309 reacting 2.5 mL of 7 mM ABTS stock solution with 44 µL of 2.5 mM potassium persulfate, allowing
310 the mixture to stand in the dark at room temperature for 16 h before use. The ABTS$^{\bullet+}$ solution (1
311 mL) was diluted with 70 mL of 5 mM phosphate buffer (pH 7.4) to an absorbance of 0.700 ± 0.002
312 at 734 nm. The reaction mixture was placed in 96-well microplates containing 10 µL
313 sample/standard and 300 µL of reagent; then the reaction was incubated in the dark at room
314 temperature for 45 min. The absorbance was measured at 734 nm using a microplate reader (Synergy
315 HT, BioTek Instruments, Winooski, VT, USA) controlled by Gen5 software (Gen5 v. 2.04 BioTek
316 Inst. Inc). Appropriate solvent blanks were run in each assay. A Trolox calibration curve (0.48 – 125

317 μM; r^2 = 0.99) was used to calculate the radical scavenging ability. Results are expressed as μmol
318 Trolox equivalents / μmol of sample

319 **Statistical Analysis**

320 All determinations were carried out at least three times, and data were expressed as the mean ±
321 standard deviation. Statistical analysis was done using GraphPad Prism V. 6.0 (GraphPad Soft. Inc.,
322 La Jolla, California, USA). One-way ANOVA and Tukey´s significance difference *post hoc* test at
323 5% level of significance by IBM SPSS Statistics version 25 (IBM Corporation, New York) were
324 performed.

325 # RESULTS & DISCUSSION

326 The effectiveness of colloidal delivery systems depends on their ability to effectively
327 encapsulate, retain, stabilize, and release bioactive compounds.[31] The performance of liposome-
328 based delivery systems depends on their composition, size, surface charge, and stability, as well as
329 the location of the bioactives within their structure.[17] For this reason, we examined the impact of the
330 initial composition and preparation method on the stability and functionality of bioactive-loaded
331 liposomes.

332 **Optimization of liposome preparation**

333 Initially, two liposome fabrication technologies that operate on different physicochemical
334 principles were assessed: microfluidization and sonication. The main goals of this part of the study
335 were to generate small liposomes, narrow particle size distributions (PSD), uniform dispersions,
336 extended shelf life, and good oxidative stability. Liposomes were prepared using these two methods
337 by dispersing 1% lecithin in sodium acetate-acetic acid buffer at pH 3.0 ± 0.1 using: (a)
338 microfluidization at 20,000 psi for different numbers of passes and (b) sonication at several
339 amplitudes and treatment times.

340 *Preparation of liposomes*

341 Figure S1 compares the PSDs of the liposome suspensions obtained using the two fabrication
342 technologies. Overall, both methods produced anionic liposomes with dimensions in the nano-scale.
343 However, the PSDs of the liposome suspensions were very broad, exhibiting multiple peaks, whose
344 size and location depended on the homogenization conditions used. None of the homogenization
345 conditions used produced a monomodal PSD, which could be due to the nature of the lecithin and/or
346 solution conditions used.

347 For microfluidization, even one pass through the homogenizer gave a large decrease in mean
348 particle diameter, *i.e.,* from 906 nm for the non-homogenized liposomes to 45.8 nm after 1 pass. The
349 mean particle diameter then decreased slightly with increasing number of passes, but remained
350 relatively constant after 5 passes.

351 For sonication, pulse intensity and treatment time affected the efficiency of liposome formation.
352 Initially, the impact of pulse amplitude (50, 60, and 75%) was studied using 10 s on/off pulses
353 applied for different treatment times. To avoid bubble formation and foaming, the sonicator tip had
354 to be submerged 1 cm from the bottom of a container to allow proper circulation and mixing of the
355 sample throughout homogenization. The results showed that overheating ($T \geq 40$ ºC) of the samples
356 could be avoided using a combination of high intensity and low treatment time. For instance, a mean
357 droplet diameter of 42.5 nm was obtained applying a pulse intensity of 75% for 4 minutes.

358 A polydispersity index ≤ 0.4 was obtained for all formulations using both sonication and
359 microfluidization. Our findings are in agreement with previous studies where microfluidization[32]
360 or sonication[33] were used to form liposomes.

Influence of preparation of liposomes on encapsulation efficiency

As mentioned above, effective preparation was achieved with: (a) microfluidizer at 20,000 psi for 5 cycles and (b) sonication at 75% for 7 min (10 s on /off pulses). After preparation using these conditions, liposomes (1.0% lecithin) with and without a model compound (125 μM EC) were incubated at 55 ºC and the encapsulation efficiency and susceptibility to lipid oxidation were measured. The same lag phase for oxidation (4 days) was observed for the control liposomes in both systems (Table 1). However, when the bioactive compound was loaded into the liposomes, the lag phase was slightly longer for sonication than microfluidization. This may have been because of their slightly higher encapsulation efficiency. Both fabrication techniques produced fairly similar mean particle diameters (50.7 – 62.2 nm) and ζ-potential values (-32.4 to -37.3 mV). The absence or presence of antioxidant did not significantly affect the ζ-potential of the liposomes, which was also reported in previous studies by Toro-Uribe et al.[17] and Gibis et al.[34] Nevertheless, the mean particle diameter of EC-loaded liposomes was higher than that of unloaded liposomes, which can be explained by the fact that phenolic compounds might be absorbed onto the surface of the lipid bilayers and/or incorporated into the core. Moreover, phenolic compounds can participate in both hydrophilic and hydrophobic interactions with the carrier system, which may impact its dimensions.[34]

Impact of the concentration of lecithin on encapsulation efficiency

To determine the most suitable ratio of lecithin-to-core material to enhance the encapsulation efficiency (EE), four concentrations of soy lecithin (1, 3, 5 and 10% wt.) were tested. In this study, the presence of cholesterol (widely used for the preparation of liposomes) was not considered. Although many studies use cholesterol as a stabilizer and to reduce bilayer permeability, other works showed that the presence of cholesterol cause limited space for the incorporation of compounds due to the steric hindrance provided by this steroid, thereby reducing the EE and affecting the release

385 rate profile.[35] Our results showed that higher EE was obtained by increasing the level of
386 phospholipids present, but at the highest concentration assayed (10%), the liposome suspension
387 behaved as a prooxidant with a lag phase of only 2 days. The highest EE was achieved using 5%
388 soy lecithin; for instance, their incorporation into liposomes increased from 27.0 to 44.7% for
389 sonication and from 18.0 to 38.6% for microfluidization (Table 1). In fact, Dag & Oztop[36] reported
390 than microfluidization was less effective in incorporating polyphenolic compounds, although the
391 liposomes produced were relatively stable to aggregation and fusion during storage. Moreover,
392 Chung[37] found that a higher ratio of encapsulated material affected the mean particle size and
393 encapsulation efficiency of liposomes produced by microfluidization, being around 1.1% lower
394 when the ratio increased from 1:4 to 1:5.

395 Based on these results, sonication at an amplitude of 75% was applied for 7 min for all further
396 studies. Besides, sonication requires less sample (no loss during processing), a lower processing
397 time, and therefore, lower energy and production costs.

398 *Influence of pH on physical stability*

399 The mean particle diameter and ζ-potential of the liposomes depended on pH (Figure S2). A
400 high stability to aggregation and phase separation was achieved from pH 3 to 5, while highly
401 unstable liposomes were obtained at pH 2 and at pH ≥ 8. These phenomena can be explained by the
402 fact that the acid/basic environment surrounding the liposomes impacts the electrostatic,
403 hydrophilic, and hydrophobic interactions in the system, thereby influencing the interfacial rheology
404 and permeability of the bilayer membrane, the aggregation state, and the encapsulation efficiency
405 of the system.[38,39] Previously, Sabín et al.[38] reported that at pH values ranging from 3 to 5 the osmotic
406 balance across phospholipid membranes is enhanced. The largest vesicles were formed at pH 2,
407 which is close to the measured isoelectric point (Figure S2). A highly acidic environment contributes
408 to a larger particle size because the anions (permeability coefficient, $P \approx 10^{-11}$-10^{-12}) are more

409 permeable than water ($P \approx 10^{-3}$-10^{-4}).[38] Moreover, the electrostatic repulsion between neighboring
410 liposomes is reduced. No dependence between particle size and ζ-potential was observed at pH
411 values ranging from 6 to 10, in which the surface potential of the liposomes was unchanged but the
412 particle size was variable.

413 Based on these results, liposome suspensions at pH 3.0 and 5.0 were selected for further study
414 because of their good stability. As can be seen in Figures S3A and S3B, the oxidative stability of
415 EC-loaded liposomes was much higher than non-loaded liposomes, thus demonstrating the
416 antioxidant activity of the polyphenol-loaded liposomes. However, the formulations at pH 5.0 were
417 more stable. For instance, the lag phase for hydroperoxide formation was 2 and 8 days the lag phase
418 for hexanal formation was 8 and 11 days for EC-loaded liposomes at pH 3.0 and 5.0, respectively.
419 In addition, the encapsulation efficiency was 2.8% higher at pH 5 than pH 3. Based on our results,
420 better encapsulation efficiency and oxidative stability, a lower particle size, and high ζ-potential
421 values were obtained at pH 5.0. Therefore, sodium acetate-acetic acid buffer at pH 5.0 was used for
422 further studies.

423 *Stability of liposomes*

424 The long-term stability of empty and EC-loaded liposomes was determined by analyzing
425 changes in their mean particle diameter, ζ-potential, pH, color, and hexanal formation over time (pH
426 5.0 ± 0.1). These parameters were chosen as good indicators of the physical and oxidative stability
427 of the liposomes. The original color of the liposome suspensions was translucid-yellow but as soon
428 as lipid oxidation occurred, the samples became turbid, which led to appreciable changes in their
429 color coordinates (L*, a*, b*). For instance, the ΔE values equal to 22.4 and 17.1, and ΔC* values
430 equal to 18.0 and 13.5 were observed for empty and EC-loaded liposomes, respectively. These
431 phenomena can be explained because during lipid oxidation the amines interacted with the aldehyde
432 products forming yellow-brown pigments as a result of non-enzymatic browning reactions.[40]

For the samples stored at 55, 37, 32, and 4 ºC, the lag phases were 3, 4, 18, and 150 days for controls and 11, 13, 30 and 210 days for EC-loaded liposomes, respectively (Figure 1). Before lipid oxidation, no aggregation or sedimentation was observed during storage, which demonstrates the good physicochemical stability of the liposome formulations as well as adequate preparation. Furthermore, EC-loaded liposome samples were lysed and analyzed by UHPLC-DAD. The results showed that 50% of the epicatechin (Figure 1C) remained after about 5 days, which confirmed that once the antioxidant was absent, lipid oxidation occurred, leading to the maximum formation of primary and secondary reaction products. Once the system was oxidized, there was a change in the mean particle diameter (74.0 ± 0.0 to 167 ± 2.8 nm, and 73.9 ± 1.3 to 177 ± 3.5), ζ-potential (-17.5 ± 0.1 to -37.3 ± 1.4, and -20.0 ± 1.33 to -38.9 ± 0.4), and pH (5.0 ± 0.1 to 5.34 ± 0.1, and 5.0 ± 0.1 to 5.26 ± 0.2) for the non-loaded and epicatechin-loaded liposomes (55 ºC), respectively. The remarkable increase in the particle size and significant reduction in ζ-potential are in agreement with the results of Chung et al.[37] who reported that this phenomenon is mainly due to the swelling of the liposomes and the formation of a complex macromolecular structure with changes in the surface properties under acidic conditions.

Simulated in vitro gastrointestinal digestion of liposomes

The main aim of these experiments was to investigate the bioaccessibility and kinetic release profiles of liposomes loaded with the studied compounds and to compare these parameters with those attainable for the bioactive compounds simply dispersed in aqueous solutions. Liposome samples were therefore prepared based on the optimum conditions established in previous sections: sonication at an intensity of 75% for 7 min; 5 wt.% soy lecithin; pH 5.0 ± 0.1; 0.1 M ionic strength. Free and liposome-loaded theobromine, caffeine, catechin, epicatechin, and cocoa extract were then incubated with simulated oral, gastric, and small intestine digestion fluids. The physicochemical properties and stability of the bioactive compounds and liposome formulations were then measured.

Electrical charge of liposomes

The ζ-potential of the initial liposomes were -15.7, -15.3, -18.7, -20.0, and -22.9 mV, for theobromine, caffeine, catechin, epicatechin, and cocoa extract, respectively (Table 1). The strong negative charge on the liposomes (Figure S2) can be attributed to the presence of charged phosphate groups.[38]

After the mouth phase, there was a slight change in the electrical charge on the liposomes being -11.8, -11.1, -15.7, -15.9, and -17.2 mV for theobromine-, caffeine-, catechin-, epicatechin-, and cocoa extract-loaded liposomes, respectively (Figure 2A). This may be due to the interaction of mucin with the liposome surfaces, which reduced the surface potential through electrostatic screening and binding effects.[12]

After the gastric phase, the magnitudes of the ζ-potentials on the liposomes became close to zero for all samples (Figure 2A). These changes can be attributed to the high ionic strength of the *in vitro* gastric phase, as well as the highly acidic gastric fluids that impacts the ionization state and charge distribution of the phosphatidylcholine heads, which agreed with Sulkwski et al.[39]

After the duodenal phase, an increase in the magnitude of the negative charge on the particles in the digested liposome suspensions was observed. For instance, the ζ-potential was -10.5, -9.5, -9.7, -9.2, and -12.3 mV for theobromine-, caffeine-, catechin-, epicatechin-, and cocoa extract-loaded liposomes, respectively. Previously, Zhang[12] reported that an increasing magnitude of the negative charge is due to the presence of various types of anionic particles in the digesta, including bile salts, micelles, vesicles, phospholipids, free fatty acids, and undigested lipid droplets. Interestingly, no noticeable difference in the electrical surface charges for all the liposome formulations ($p < 0.05$) were observed, which indicates that the differences during the *in vitro* gastrointestinal assays are related to the nature of the soy liposomes instead of the encapsulated compound.

Particle size and microstructure

To better understand how the liposome membrane was affected within the *in vitro* gastrointestinal tract, the particle size was determined by light scattering and the microstructure was determined by TEM and confocal microscopy. Figure 3 summarizes the proposed mechanism of release and transformation of liposomes within simulated digestive fluids. Morphological changes from spherical to oval shape, swelling, interaction with digestive components, and perturbation of the membrane are suggested to account for the observed effects based on the results obtained in the present study. Further details are given below.

Figure 2B shows that the lowest particle size was obtained for all the samples before digestion. More insight is provided by the TEM images (Figure 4 A-D), where it can be clearly observed that vesicles were semi-spherical with similar particle size distributions, which agrees with our dynamic light scattering study. Therefore, non-loaded liposomes together with theobromine-, epicatechin-, and cocoa extract-loaded liposomes with cross section vesicle lengths between 40-90, 80-130, 70-130, and 30-115 nm, respectively, were formed. Interestingly, honeycomb- or cluster-like structures consistent with the presence of circular interlayer contacts[41] were observed. A slight increase of the hydration layer by around 1.0, 1.0, 1.2, and 1.5-2.0 nm for non-loaded, theobromine-, epicatechin- and cocoa extract-loaded liposomes respectively, were seen. These data confirmed the interaction of the compounds having different polarities with the lipid bilayer, in particular for the cocoa extract. Analysis of the surface morphology of the vesicles indicated that all the formulations contained bilayer hetero-junctions with similar inter-layer thicknesses from 3 to 7 nm. Nevertheless, the average number of bilayers per liposome appeared to be affected by the nature of the encapsulated compound. For instance, it was observed that non-loaded and Theo-loaded liposomes preferably formed single bilayer, while EC-loaded liposomes were multilayered. Overall, the bilayer surfaces had very smooth and thin appearances, with regular curved edges. Solubility-diffusion theory

505 considers the bilayer membrane to be a homogeneous slab of bulk organic material through which
506 the permeant must partition into and diffuse across.[42] Moreover, the capture volume was smaller for
507 the empty liposomes, followed by Theo-loaded liposomes, and being highest for EC- and cocoa
508 extract-loaded liposomes. These findings suggest that the level of entrapped compounds into the
509 core (EE catechins >>> alkaloids) may play a role in the vesicle formation process. Thus, liposome
510 size is a determining factor for permeability and may affect the release rate.[38]

511 Electron and confocal microscopy images suggested no appreciable difference in the mean
512 particle size of the liposomes within the mouth phase (Figure 2B, Figure S4 E-G, and Figure 4 E-
513 G). However, in Figure S4F, slight differences on particle size as a consequence of the interaction
514 of polyphenol compounds with α-amylase are visible, which have been previously explained by
515 Xiao.[43] Extensive agglomeration changes of morphological structure forming larger vesicles and
516 greater core volume into the liposome were observed in Figure S4 I-L and Figure 4 I-L. This may
517 be due to the addition of HCl to the medium, that can change phospholipid permeability and osmotic
518 pressure,[38] leading to liposome swelling. In fact, Figure 2B shows that during the gastric phase, the
519 increase of particle size diameter was 1650 ± 40, 1540 ± 170, 1380 ± 340, 1240 ± 260, and 2400 ±
520 380 nm, for Theo-, Caf-, C-, EC-, and cocoa extract-loaded liposomes, respectively. Despite all these
521 changes, lysis or membrane disruption were not observed suggesting that a controlled release profile
522 could be achieved throughout the digestion transit time.

523 Interestingly, at a later stage, when the sample moved from the stomach to the small intestine
524 (Figure 4 M-P), a significant reduction in the number of bilayers was observed, which would be
525 expected to impact the molecular diffusion process. Moreover, there was a breakage of the interlayer
526 junctions causing evident changes on lipid-bilayer (e.g., reduction of number of bilayers) as well as
527 heterogeneous morphological shape and size of liposomes. All these factors favored the released of
528 the encapsulated compounds. Moreover, at the end of the duodenal phase, the size of the liposomes

529 decreased, which was confirmed by dynamic light scattering and confocal microscopy images
530 (Figure 2B and Figure S4 M-P). Unfortunately, it proved to be difficult to obtain good images of
531 these samples by TEM.

532 The observed reduction of particle size in the small intestine could have occurred for a number
533 of reasons. Firstly, the added Na^+ ions modified the osmotic forces; liposomes react to this change
534 by evacuating water from their insides to compensate for the excess of cations outside of them, thus
535 causing them to decrease in diameter.[38] Secondly, cationic ions adsorbed to the bilayers (e.g., K^+,
536 Na^+, and Ca^{2+}) and altered their interactions and optimum curvature. Thirdly, bile salts entered the
537 phospholipid bilayers and disrupted the liposome structure. Fourthly, the fatty acids released from
538 digestion of the phospholipids were solubilized in the mixed micelles. These findings are in line
539 with those reported by Zhang[12] who observed that lipid droplets were digested by lipase molecules,
540 resulting in the formation of free fatty acids, vesicles, monoacylglycerols, and mixed micelles.
541 Indeed, a lower fluorescence signal was observed at the end of digestion, which indicates that the
542 oil phase had been digested by lipase (Figure S4 M-P). These results are consistent with the free
543 fatty acid profiles (data not shown), where the measurement of the volume of NaOH required to
544 keep the pH equal to 7.0 was relatively constant for 6 h in simulated small intestine, that is, almost
545 complete digestion of lipids were achieved.

546 *Comparison of the simulated in vitro digestion of loaded liposomes (model system) vs. free*
547 *bioactive compounds*

548 The concentration of each bioactive compound during digestion was determined by collecting
549 aliquots at several time points that were analyzed by UHPLC-DAD. Overall, all the formulations
550 (free and liposome-loaded bioactives) were highly stable during the simulated oral phase, as a
551 consequence of the short residence time (2 min). On the other hand, significant differences among

552 free and encapsulated bioactives were observed, confirming that the nature of the compound, carrier,
553 and encapsulation efficiency impacted bioactive release.

554 During the gastric phase (0 to 2 h), alkaloids were resistant to acid hydrolysis, with the Theo-
555 loaded liposomes showing fairly similar degradation as the Caf-loaded liposomes (Figure 5 A-B).
556 At the end of the gastric phase, 100.9 ± 2.7 and 100.1 ± 3.0% free Theo and Caf still remained,
557 which were 1.37 and 1.26-fold higher than Theo-, and Caf-loaded liposomes, respectively (Figure 5
558 A-B). Regarding catechins, free C and EC were also highly stable at low pH, therefore, their
559 concentrations were only reduced by 1.5 and 0.8%, respectively (Figure 5 C-D). In comparison,
560 when C- and EC-loaded liposomes formulations were exposed to gastric phase, the lowest
561 concentrations were reached being equal to 25.6 ± 1.6 and 35.3 ± 4.5%, that is, 3.8– and 2.8– fold
562 lower than the free bioactive, respectively. These findings suggest that lower amount detected could
563 be as consequence of i) greater extent and/or transformation of catechins, ii) good performance of
564 the delivery system to protect the active ingredient from simulated gastric environment or iii) the
565 swelling effect of liposome allowing greater incorporation of bioactive into the membranes.

566 Free Theo and Caf exposed to intestinal digestion (2 to 8 h) were still stable, reducing their
567 concentration only by 20.6 and 24.9%, respectively. These results agree with Mogi et al[44] who
568 reported that plasma bioavailability was approximately 80% for caffeine up to 24 h after dosing.
569 Nevertheless, Theo- and Caf-loaded liposomes dramatically decreased to 25.2 ± 1.6 and 32.8 ± 0.7%
570 (Figure 5 A-B). As the only difference between the aqueous system and the liposome formulation
571 is the phospholipid membrane, we hypothesized that the degradation of alkaloid-loaded liposomes
572 appears to be directly correlated not only to the hydrolysis of lipids, triggered by pancreatic
573 excretions, especially the phospholipase A2 and bile salts, but also by the poor EE of theobromine
574 (0.03%) and caffeine (0.04%) rather than pH. These results might indicate that the delivery system

575 for alkaloids deserves further research, possibly by the addition of a coating layer of liposomes, and
576 better formulation, leading to better stability in the gastrointestinal system.

577 The main loss of free catechins was due to intestinal phase degradation, with reductions of ca.
578 70.6 and 77.5% for C and EC. Hence, the duodenal losses were about 70.2 and 77.3% higher than
579 the gastric phase losses, respectively (Figure 5 C-D). Therefore, the high stability under stomach
580 conditions for catechin is comparable to previously reported results *in vitro*.[9,13] Moreover,
581 epimerization of (+)-catechin → (-)-epicatechin, and (-)-epicatechin → (+)-catechin was also
582 detected. According to the literature, degradation of catechins under digestive conditions appears to
583 be directly correlated to pH rather than to digestive enzyme activity. For instance, Bouayed et al.[9]
584 evaluated the content of epicatechin from several apples varieties and reported losses during gastric
585 digestion of 19.8 – 69.8% and complete degradation in the small intestinal phase.

586 On the other hand, Figure 5 demonstrates a typical prolonged and sustained drug-release profile
587 for C- and EC-loaded liposomes. As expected, as soon as the carrier comes into contact with the
588 intestinal digestion medium, an initial burst release was observed, which could be related to the
589 release of the active ingredient adsorbed on the lipid surface or encapsulated into the core of the
590 liposomes. Thereafter, the release rate became slow and reached equilibrium during the transit time.
591 As can be observed in Figure 5 C-D, and compared to free catechins, a peak concentration for C-
592 and EC-loaded liposomes became apparent after ca. 4 and 4.6 h of digestion, respectively. Indeed,
593 higher bioaccessibilities for C (57.7 ± 3.3%)- and EC (49.2 ± 2.3%)-loaded liposomes were 2.0 and
594 2.2- fold higher than free C and EC (Table 1, $p < 0.05$), respectively. Overall, our data suggest that
595 the formulation containing catechin-loaded liposomes improved its bioaccessibility and may lead to
596 a higher bioavailability and intestinal uptake.

Comparison of the simulated in vitro digestion of cocoa extract-loaded liposomes vs. free cocoa extract.

Cocoa extract is mainly composed of alkaloids, flavan-3-ols and oligomeric procyanidins with a degree of polymerization up to 14.[25] Overall, theobromine and (-)-epicatechin constitute 13.1 and 14.5% of major alkaloids and flavan-3-ols in the cocoa extract, respectively. In this regard, trimer was the most abundant procyanidin, being equal to 22.1% of whole cocoa extract, followed by tetramer (16.7%), pentamer (13.2%), dimer (9.1%), and hexamer (6.3%).[25] Higher oligomers were detected but not quantified due to the lack of standards. In this study, the primary focus was on the *in vitro* digestion of the alkaloids and catechins present in this extract. To do so, the cocoa extract was dissolved in an aqueous system (free) as well as loaded into liposomes.

The alkaloids from the free cocoa extract were highly stable within the mouth and gastric phases. In this case, caffeine was more stable than theobromine during all three phases assayed (Figure 6 A-B). For example, the theobromine present in the free cocoa extract was 1.45 and 2.98 - fold lower than free theobromine alone in the gastric and duodenal phases, respectively. Similarly, caffeine from free cocoa extract was 1.24-fold lower than free caffeine alone in the gastric phase, and quite similar during the intestine phase, being around 75.1 and 83.5% for caffeine from free cocoa extract and from free caffeine, respectively. On the other hand, the alkaloids from the cocoa extract-loaded liposomes had worse performance for theobromine and slightly better for caffeine. Bioaccessibility for caffeine (83.5 to 31.5%, $p < 0.05$) and theobromine (26.6 to 8.4%, $p < 0.05$) from free cocoa extract was also higher than the values obtained for these compounds in the cocoa extract-loaded liposomes (Table 1). These findings rule out the considerable decomposition of theobromine, thus formation of unknown compounds or the conversion of the latter into caffeine. In addition, the highest magnitude reported for free cocoa extract alkaloids could be explained as a

result of the high dose assayed together with the effect of the food matrix which could impact their bioaccessibility and absorption.[13]

After the cocoa extract-loaded liposomes were exposed to the intestinal phase, an increasing concentration and then a sustained release profile of their bioactive compounds were detected (Figure 6 C-D). Indeed, the peak concentration of C and EC from cocoa extract-loaded liposomes become greater than those present on the free cocoa extract at about 5 and 6 h, respectively, which could be explained by lysis of the liposomes (Figure 6 C-D). Furthermore, the bioaccessibility of C and EC from cocoa extract-loaded liposomes was 2.3 and 2.2–fold higher than those from free cocoa extract (Table 1). Overall, these data highlight that liposomes may be a good carrier system to improve the *in vitro* controlled release of catechins.

DPPH· radical scavenging activity

DPPH radical scavenging activity was quantified in terms of the percentage inhibition after exposure to different phases of the gastrointestinal model (Table 2). As expected, Theo- and Caf-loaded liposomes were inefficient as antioxidants, with no significant changes due to the digestion system (similar values for non-loaded liposomes). In addition, the initial DPPH scavenging activity of alkaloids can be attributed to the presence of other compounds in the lecithin such as tocopherols (soy lecithin composed of 16.5 ± 0.6, 102.0 ± 24.9, and 1.5 ± 0.3 $mg/kg_{Lecithin}$ of β, δ, and γ tocopherols, respectively).

Higher antioxidant activities in duodenal phase for free EC, and C were 1.27- and 1.40-fold higher compared to those of gastric phases, respectively. These findings can be explained as a result of greater remaining concentration during the digestion and/or formation of autooxidation products from catechins (e.g., homodimers), which may contribute to higher antioxidant activity.[13] Catechin-loaded liposomes had the highest and lowest reduction of radical scavenging activity before digestion and during the gastric phase. The latter could be attributed to the lowest content of

644 antioxidants released into the whole system (Figure 5C-D), the lower reaction between antioxidants
645 and DPPH radical, and to the lower deprotonation at acidic pH. Significant differences were
646 observed between cocoa formulations; in general, cocoa extract-loaded liposomes had higher
647 antioxidant activity than the free extract ($p<0.05$), which could be attributed to the protection of
648 liposomes against the degradation of polyphenols. Among the samples, cocoa extract had the highest
649 antioxidant activity, which could be attributed to the presence of other non-polyphenolic compounds
650 or highly solubilized micelles that impact the activity and rate of the DPPH radical scavenging; for
651 instance, Chat[45] reported the solubilization capacity of various surfactant systems to scavenge
652 radicals increasing following the order cationic > non-ionic > anionic.

653 In general, by increasing the pH of the surrounding medium, a maximum scavenging inhibition
654 was reached. This behavior reflects that catechins are in deprotonated forms instead of neutral.
655 Therefore, upon deprotonation, the radical scavenging capacity of the catechins increases because
656 electron donation becomes much easier.[46] These data also provide more insight into the mechanism
657 (pH-sensitive liposome) underlying the ability for neutral pH and/or enzymatic action to affect the
658 liposome membrane conformation, thus, favoring the release of the encapsulated compound from
659 the inner membrane.

660 *$ABTS^{\cdot+}$ radical cation analysis*

661 Similarly, to DPPH data, alkaloids were inefficient for scavenging $ABTS^{\cdot+}$ free-radical cations.
662 In fact, Brezová et al.[47] previously reported that caffeine is inert to $ABTS^{\cdot+}$ and $DPPH^{\cdot+}$ oxidants,
663 but effective in the scavenging of $^{\bullet}OH$ radicals. According to our results, significant variations in
664 ABTS radical scavenging activity were observed, which demonstrate the effect of pH on the radical
665 scavenging capacities. Muzolf[46] verified the pH-dependent increase in the TEAC values, that is,
666 upon deprotonation of catechin, for instance, C and EC had ABTS values between 0 - 3.5 mM Trolox
667 per mM $sample^{-1}$ for pH ranging of 0 – 9.5.

As can be seen in Table 2, the ability to scavenge $ABTS^{\cdot+}$ cation radicals for free compounds rose by increasing the digestion transit time. Regarding the small intestine, differences among samples with and without liposomes were observed which could be due to nature of the bioactive compound and/or the influence of carrier system. In general, high antioxidant activity was achieved even at lower concentration of residual bioactive compound, for instance, free C and EC were 29.4 and 22.5 bioaccessible at duodenal stage. A similar trend was also found by Wootton-Beard[48] who reported that many polyphenols from several vegetable sources had a higher ABTS scavenging activity during the duodenal phase. Based on these results, it can be hypothesized that the highest ABTS radical activity was not only function of remaining compounds, but also suggested the presence of new products as a result of epimerization and oxidation of bioactive compounds.

Significant differences ($p < 0.05$) between free extract and cocoa extract-loaded liposomes were observed. As expected, the highest antioxidant activity was for cocoa extract-loaded liposomes. This phenomenon can be attributed to a number of reasons: (a) the antioxidant activity can be masked by the interaction of free flavonoids with proteins, (b) adsorption of cocoa polyphenols into the lipid phase in different magnitude (c) charge of micelles and its role on the chemical behavior of the bioactive compounds that may affect their final antioxidant value, and (d) different rate of deprotonation of phenolic hydroxyl groups at alkaline pH. For instance, deprotonation of the 3'-OH group in the catechin ($pKa = 4.6$)[49] can dissociate resulting in a mixture of neutral and anionic species, while other hydroxyls groups could be responsible for scavenging of free-radicals (e.g., 5- and 7-OH groups at A-ring, and 3-OH at C ring). It is worth to mention, the highest free radical scavenging for cocoa extract-loaded liposomes is comprehensive since the liposome system contribute at high amount of phospholipids, therefore, higher solubilized micelles. Thereby, solubilization of antioxidant compound within the Stern (hydrophilic), or Palisade (hydrophobic)

691 layer of micelles together with electrostatic forces provides a more appropriate microenvironment
692 to donate H atoms to reduce $ABTS^{\cdot+}$ into nonradical form easily.[50]

693

694 In general, the present study showed that liposomes are capable of increasing the
695 bioaccessibility of flavan-3-ols, which may be important for the development of nutraceutical-
696 enriched functional foods. Our results highlight the importance of further studies (*in vitro* and *in*
697 *vivo*) on the bioaccessibility, bioavailability and biological fate of polyphenols (e.g., polymeric
698 catechins) in both aqueous solutions and incorporated into delivery systems, as well as evaluation
699 of their releasing mechanism in real food systems.

700

701 **SUPPORTING INFORMATION**

702 Detailed list of influence of particle size distribution of both microfluidization and sonication
703 technology (Figure S1), influence of pH on the physical stability of liposomes (Figure S2), oxidative
704 stability (Figure S3), and confocal optical microscopy images for the tested samples before and after
705 *in vitro* digestion process (Figure S4) are shown in the supporting information.

706 **REFERENCES**

707 (1) Ignat, I.; Volf, I.; Popa, V. I. A Critical Review of Methods for Characterisation of Polyphenolic
708 Compounds in Fruits and Vegetables. *FOOD Chem.* **2011**, *126* (4), 1821–1835.

709 (2) Frary, C. D.; Johnson, R. K.; Wang, M. Q. Food Sources and Intakes of Caffeine in the Diets
710 of Persons in the United States. *J. Am. Diet. Assoc.* **2005**, *105* (1), 110–113.

711 (3) Gu, L.; Kelm, M. A.; Hammerstone, J. F.; Beecher, G.; Holden, J.; Haytowitz, D.; Gebhardt,
712 S.; Prior, R. L. Concentrations of Proanthocyanidins in Common Foods and Estimations of
713 Normal Consumption. *J. Nutr.* **2004**, *134* (3), 613–617.

714 (4) Watson, R.; Preedy, V. R.; Zibadi, S. *Chocolate in Health and Nutrition*; Preedy, V. R., Watson,
715 R. R., Zibadi, S., Eds.; Humana Press: New York, NY, 2012.

716 (5) Eteng, M. U.; Eyong, E. U.; Akpanyung, E. O.; Agiang, M. A.; Aremu, C. Y. Recent Advances
717 in Caffeine and Theobromine Toxicities: A Review. *Plant Foods Hum. Nutr.* **1997**, *51* (3),
718 231–243.

719 (6) Cirillo, G.; Curcio, M.; Vittorio, O.; Iemma, F.; Restuccia, D.; Spizzirri, U. G.; Puoci, F.; Picci,
720 N. Polyphenol Conjugates and Human Health: A Perspective Review. *Crit. Rev. Food Sci.*
721 *Nutr.* **2016**, *56* (2), 326–337.

722 (7) Kumar, S.; Pandey, A. K. Chemistry and Biological Activities of Flavonoids: An Overview.
723 *Sci. World J.* **2013**, *1* (1), 1–16.

724 (8) Fang, Z.; Bhandari, B. Encapsulation of Polyphenols - a Review. *Trends Food Sci. Technol.*
725 **2010**, *21* (10), 510–523.

726 (9) Bouayed, J.; Deußer, H.; Hoffmann, L.; Bohn, T. Bioaccessible and Dialysable Polyphenols in
727 Selected Apple Varieties Following in Vitro Digestion vs. Their Native Patterns. *Food Chem.*

728 **2012**, *131* (4), 1466–1472.

729 (10) Ovando-Martínez, M.; Gámez-Meza, N.; Molina-Domínguez, C. C.; Hayano-Kanashiro, C.;
730 Medina-Juárez, L. A. Simulated Gastrointestinal Digestion, Bioaccessibility and Antioxidant
731 Capacity of Polyphenols from Red Chiltepin (Capsicum Annuum L. Var. Glabriusculum)
732 Grown in Northwest Mexico. *Plant Foods Hum. Nutr.* **2018**, *73* (2), 116–121.

733 (11) Lee, M.; Maliakal, P.; Chen, L.; Meng, X.; Bondoc, F. Pharmacokinetics of Tea Catechins
734 after Ingestion of Green Tea and (−)-Epigallocatechin-3-Gallate by Humans — Cancer
735 Epidemiology, Biomarkers & Prevention. *Cancer Epidemiol.* **2002**, *11* (10), 1025–1032.

736 (12) Zhang, R.; Zhang, Z.; Zou, L.; Xiao, H.; Zhang, G.; Decker, E. A.; McClements, D. J.
737 Enhancing Nutraceutical Bioavailability from Raw and Cooked Vegetables Using Excipient
738 Emulsions: Influence of Lipid Type on Carotenoid Bioaccessibility from Carrots. *J. Agric.*
739 *Food Chem.* **2015**, *63* (48), 10508–10517.

740 (13) Neilson, A. P.; Ferruzzi, M. G. Influence of Formulation and Processing on Absorption and
741 Metabolism of Flavan-3-Ols from Tea and Cocoa. *Annu. Rev. Food Sci. Technol.* **2011**, *2* (1),
742 125–151.

743 (14) Ferreira, I.; Rocha, S.; Coelho, M. Encapsulation of Antioxidants by Spray-Drying. *Chem.*
744 *Eng. Trans.* **2007**, *11*, 713–718.

745 (15) Belščak-Cvitanović, A.; Stojanović, R.; Manojlović, V.; Komes, D.; Cindrić, I. J.; Nedović,
746 V.; Bugarski, B. Encapsulation of Polyphenolic Antioxidants from Medicinal Plant Extracts
747 in Alginate-Chitosan System Enhanced with Ascorbic Acid by Electrostatic Extrusion. *Food*
748 *Res. Int.* **2011**, *44* (4), 1094–1101.

749 (16) Paximada, P.; Echegoyen, Y.; Koutinas, A. A.; Mandala, I. G.; Lagaron, J. M. Encapsulation

of Hydrophilic and Lipophilized Catechin into Nanoparticles through Emulsion Electrospraying. *Food Hydrocoll.* **2017**, *64*, 123–132.

(17) Toro-Uribe, S.; López-Giraldo, L. J.; Decker, E. A. Relationship between the Physiochemical Properties of Cocoa Procyanidins and Their Ability to Inhibit Lipid Oxidation in Liposomes. *J. Agric. Food Chem.* **2018**, *66* (17), 4490–4502.

(18) Bhushani, J. A.; Karthik, P.; Anandharamakrishnan, C. Nanoemulsion Based Delivery System for Improved Bioaccessibility and Caco-2 Cell Monolayer Permeability of Green Tea Catechins. *Food Hydrocoll.* **2016**, *56*, 372–382.

(19) Aditya, N. P.; Aditya, S.; Yang, H. J.; Kim, H. W.; Park, S. O.; Lee, J.; Ko, S. Curcumin and Catechin Co-Loaded Water-in-Oil-in-Water Emulsion and Its Beverage Application. *J. Funct. Foods* **2015**, *15*, 35–43.

(20) Altin, G.; Gültekin-Özgüven, M.; Ozcelik, B. Chitosan Coated Liposome Dispersions Loaded with Cacao Hull Waste Extract: Effect of Spray Drying on Physico-Chemical Stability and in Vitro Bioaccessibility. *J. Food Eng.* **2018**, *223*, 91–98.

(21) Lee, J. S.; Chung, D.; Lee, H. G. Preparation and Characterization of Calcium Pectinate Gel Beads Entrapping Catechin-Loaded Liposomes. *Int. J. Biol. Macromol.* **2008**, *42* (2), 178–184.

(22) Yadav, A. V.; Murthy, M. S.; Shete, A. S.; Sakhare, S. Stability Aspects of Liposomes. *Indian J. Pharm. Educ. Res.* **2011**, *45* (4), 402–413.

(23) Panya, A.; Laguerre, M.; Lecomte, J.; Villeneuve, P.; Weiss, J.; McClements, D. J.; Decker, E. A. Effects of Chitosan and Rosmarinate Esters on the Physical and Oxidative Stability of Liposomes. *J. Agric. Food Chem.* **2010**, *58* (9), 5679–5684.

772 (24) Yang, S. B.; Liu, C. M.; Liu, W.; Yu, H.; Zheng, H. J.; Zhou, W.; Hu, Y. Preparation and
773 Characterization of Nanoliposomes Entrapping Medium-Chain Fatty Acids and Vitamin C
774 by Lyophilization. *Int. J. Mol. Sci.* **2013**, *14* (10), 19763–19773.

775 (25) Toro-Uribe, S.; Montero, L.; López-Giraldo, L.; Ibáñez, E.; Herrero, M. Characterization of
776 Secondary Metabolites from Green Cocoa Beans Using Focusing-Modulated Comprehensive
777 Two-Dimensional Liquid Chromatography Coupled to Tandem Mass Spectrometry. *Anal.*
778 *Chim. Acta* **2018**, *(in press)*, 1–10.

779 (26) Hu, M.; McClements, D. J.; Decker, E. A. Lipid Oxidation in Corn Oil-in-Water Emulsions
780 Stabilized by Casein, Whey Protein Isolate, and Soy Protein Isolate. *J. Agric. Food Chem.*
781 **2003**, *51* (6), 1696–1700.

782 (27) Qian, C.; Decker, E. A.; Xiao, H.; Mcclements, D. J. Nanoemulsion Delivery Systems :
783 Influence of Carrier Oil on b -Carotene Bioaccessibility. *Food Chem.* **2012**, *135* (3), 1440–
784 1447.

785 (28) Minekus, M.; Alminger, M.; Alvito, P.; Ballance, S.; Bohn, T.; Bourlieu, C.; Carrière, F.;
786 Boutrou, R.; Corredig, M.; Dupont, D.; et al. A Standardised Static in Vitro Digestion Method
787 Suitable for Food – an International Consensus. *Food Funct.* **2014**, *5* (6), 1112–1113.

788 (29) Brand-Williams, W.; Cuvelier, M. E.; Berset, C. Use of a Free Radical Method to Evaluate
789 Antioxidant Activity. *LWT Food Sci ence Technol.* **1995**, *28* (1), 25–30.

790 (30) Re, R.; Pellegrini, N.; Proteggente, A.; Pannala, A.; Yang, M.; Rice-Evans, C. Antioxidant
791 Activity Applying an Improved ABTS Radical Cation Decolorization Assay. *Free Radic.*
792 *Biol. Med.* **1999**, *26* (9–10), 1231–1237.

793 (31) McClements, D. J. *Nanoparticle- and Microparticle-Based Delivery Systems: Encapsulation,*

794 *Protection and Release of Active Compounds*; Taylor & Francis Group: Boca Raton, FL,
795 2014.

796 (32) Lajunen, T.; Hisazumi, K.; Kanazawa, T.; Okada, H.; Seta, Y.; Yliperttula, M.; Urtti, A.;
797 Takashima, Y. Topical Drug Delivery to Retinal Pigment Epithelium with Microfluidizer
798 Produced Small Liposomes. *Eur. J. Pharm. Sci.* **2014**, *62*, 23–32.

799 (33) Silva, R.; Ferreira, H.; Little, C.; Cavaco-Paulo, A. Effect of Ultrasound Parameters for
800 Unilamellar Liposome Preparation. *Ultrason. Sonochem.* **2010**, *17* (3), 628–632.

801 (34) Gibis, M.; Vogt, E.; Weiss, J. Encapsulation of Polyphenolic Grape Seed Extract in Polymer-
802 Coated Liposomes. *Food Funct.* **2012**, *3* (3), 246–254.

803 (35) Briuglia, M. L.; Rotella, C.; McFarlane, A.; Lamprou, D. A. Influence of Cholesterol on
804 Liposome Stability and on in Vitro Drug Release. *Drug Deliv. Transl. Res.* **2015**, *5* (3), 231–
805 242.

806 (36) Dag, D.; Oztop, M. H. Formation and Characterization of Green Tea Extract Loaded
807 Liposomes. *J. Food Sci.* **2017**, *82* (2), 463–470.

808 (37) Chung, S. K.; Shin, G. H.; Jung, M. K.; Hwang, I. C.; Park, H. J. Factors Influencing the
809 Physicochemical Characteristics of Cationic Polymer-Coated Liposomes Prepared by High-
810 Pressure Homogenization. *Colloids Surfaces A Physicochem. Eng. Asp.* **2014**, *454* (1), 8–15.

811 (38) Sabín, J.; Prieto, G.; Ruso, J. M.; Hidalgo-Álvarez, R.; Sarmiento, F. Size and Stability of
812 Liposomes: A Possible Role of Hydration and Osmotic Forces. *Eur. Phys. J. E* **2006**, *20* (4),
813 401–408.

814 (39) Sułkowski, W. W.; Pentak, D.; Nowak, K.; Sułkowska, A. The Influence of Temperature,
815 Cholesterol Content and PH on Liposome Stability. *J. Mol. Struct.* **2005**, *744–747* (SPEC.

ISS.), 737–747.

(40) Thanonkaew, A.; Benjakul, S.; Visessanguan, W.; Decker, E. A. Yellow Discoloration of the Liposome System of Cuttlefish (Sepia Pharaonis) as Influenced by Lipid Oxidation. *Food Chem.* **2007**, *102* (1), 219–224.

(41) Polozova, A.; Li, X.; Shangguan, T.; Meers, P.; Schuette, D. R.; Ando, N.; Gruner, S. M.; Perkins, W. R. Formation of Homogeneous Unilamellar Liposomes from an Interdigitated Matrix. *Biochim. Biophys. Acta - Biomembr.* **2005**, *1668* (1), 117–125.

(42) Maherani, B.; Arab-Tehrany, E.; Kheirolomoom, A.; Geny, D.; Linder, M. Calcein Release Behavior from Liposomal Bilayer; Influence of Physicochemical/Mechanical/Structural Properties of Lipids. *Biochimie* **2013**, *95* (11), 2018–2033.

(43) Xiao, J.; Kai, G.; Ni, X.; Yang, F.; Chen, X. Interaction of Natural Polyphenols with α-Amylase in Vitro: Molecular Property-Affinity Relationship Aspect. *Mol. Biosyst.* **2011**, *7* (6), 1883–1890.

(44) Mogi, M.; Toda, A.; Iwasaki, K.; Kusumoto, S.; Takehara, H.; Shimizu, M.; Murayama, N.; Izumi, H.; Utoh, M.; Yamazaki, H. Simultaneous Pharmacokinetics Assessment of Caffeine, Warfarin, Omeprazole, Metoprolol, and Midazolam Intravenously or Orally Administered to Microminipigs. *J. Toxicol. Sci.* **2012**, *37* (6), 1157–1164.

(45) Chat, O. A.; Najar, M. H.; Mir, M. A.; Rather, G. M.; Dar, A. A. Effects of Surfactant Micelles on Solubilization and DPPH Radical Scavenging Activity of Rutin. *J. Colloid Interface Sci.* **2011**, *355* (1), 140–149.

(46) Muzolf, M.; Szymusiak, H.; Gliszczynska-Swiglo, A.; Rietjens, I. M. C. M.; Tyrakowska, B. PH-Dependent Radical Scavenging Capacity of Green Tea Catechins. *J. Agric. Food Chem.*

838 **2008**, *56* (3), 816–823.

839 (47) Brezová, V.; Šlebodová, A.; Staško, A. Coffee as a Source of Antioxidants: An EPR Study.
840 *Food Chem.* **2009**, *114* (3), 859–868.

841 (48) Wootton-Beard, P. C.; Moran, A.; Ryan, L. Stability of the Total Antioxidant Capacity and
842 Total Polyphenol Content of 23 Commercially Available Vegetable Juices before and after
843 in Vitro Digestion Measured by FRAP, DPPH, ABTS and Folin-Ciocalteu Methods. *Food*
844 *Res. Int.* **2011**, *44* (1), 217–224.

845 (49) Jovanovic, S. V.; Steenken, S.; Tosic, M.; Marjanovic, B.; Simic, M. G. Flavonoids as
846 Antioxidants. *J. Am. Chem. Soc.* **1994**, *116* (11), 4846–4851.

847 (50) Wu, Y.; Wang, X. Binding, Stability, and Antioxidant Activity of Curcumin with Self-
848 Assembled Casein–dextran Conjugate Micelles. *Int. J. Food Prop.* **2017**, *20* (12), 3295–3307.

FUNDING

S.T.U. wants to thank Colciencias-Colombia for financial support, and Universidad Industrial of Santander (Colombia), University of Massachusetts (Food Science Department, USA) and Instituto de Investigación en Ciencias de la Alimentación (CIAL, Spain) for making this work possible. Authors thank Project AGL2017-89417-R (MINECO, Spain) for financial support.

FIGURE CAPTIONS

Figure 1. Time to lipid oxidation determined by hexanal formation for (A) non-loaded liposomes, (B) epicatechin-loaded (EC, 125 μM) liposomes, and (C) epicatechin-loaded liposome release over time (stored at 55 °C).

Figure 2. ζ-potentials (A) and mean particle size (B) of compounds-loaded liposomes before and after each simulated *in vitro* digestion step. Samples with different capital letters (A, B, C) indicate significant differences ($p<0.05$) between same digestion phases for the different bioactive compounds. Samples designated with different lower-case letters (a, b, c, d) were significantly different ($p< 0.05$) between different digestion phases for the same bioactive compounds.

Figure 3. Suggested mechanisms of physicochemical changes of liposomes before and after simulated gastrointestinal digestion.

Figure 4. TEM images of (A) non-loaded and (B) theobromine-, (C), epicatechin-, and (D), cocoa extract-loaded liposomes, before and after physicochemical changes produced during simulated *in vitro* gastrointestinal digestion.

Figure 5. Stability profile under simulated *in vitro* conditions of free and liposome-loaded (A) theobromine, (B) caffeine, (C) catechin, and (D) epicatechin.

Figure 6. Concentration remaining under simulated *in vitro* digestion of (A) theobromine, (B) caffeine, (C) catechin, and (D) epicatechin from free extract and cocoa extract-loaded liposomes.

1

Table 1. Physiochemical Parameters and Bioaccessibility of Liposome Samples for the Designed Process and During Simulated *In Vitro* GIT Digestion.

	Lecithin (wt %)	pH	Concentration (μM)	Lag phase (day)	Mean size (nm)	ζ-potential (mV)	Encapsulation Efficiency (%)	Bioaccessibility (%)
Microfluidization (20 Kpsi, 5 passes) *								
- Control Liposome	1	3.0	-	4	59.07 ± 3.90^{a}	-36.80 ± 2.69^{a}	-	-
- Epicatechin Liposomal	1	3.0	125	5	62.24 ± 0.57^{a}	-32.40 ± 3.54^{a}	18.04 ± 0.03^{a}	-
- Epicatechin Liposomal*	5	3.0	125	6	59.07 ± 3.90^{a}	-36.80 ± 2.69^{a}	38.56 ± 0.20^{b}	-
Sonication (75% amplitude, 7 min) *								
- Control Liposome	1	3.0	-	4	50.75 ± 7.86^{a}	-37.30 ± 1.98^{a}	-	-
- Epicatechin Liposomal	1	3.0	125	6	53.09 ± 4.53^{a}	-35.35 ± 8.41^{a}	27.02 ± 0.02^{a}	-
- Control Liposome	5	3.0	-	3	56.71 ± 1.49^{a}	-31.50 ± 0.28^{a}	-	-
- Epicatechin Liposomal	5	3.0	125	8	52.32 ± 6.10^{a}	-32.45 ± 0.37^{a}	44.70 ± 0.02^{b}	-
Formulation at pH 5.0 loaded liposomes								
- Control Liposome	5	5.0	-	8	74.03 ± 0.01^{a}	$-17.50 \pm 0.08^{a,b,c}$	-	-
- Theobromine Liposomal	5	5.0	1000	-	75.72 ± 1.48^{a}	$-15.70 \pm 1.70^{b,c}$	0.03 ± 0.02^{a}	$35.86 \pm 2.48^{a,A}$
- Caffeine Liposomal	5	5.0	1000	-	75.66 ± 0.18^{a}	-15.25 ± 0.78^{c}	0.04 ± 0.03^{a}	$39.40 \pm 1.61^{a,A}$
- Catechin Liposomal	5	5.0	1000	-	79.46 ± 0.58^{b}	$-18.70 \pm 0.57^{a,b}$	46.66 ± 3.89^{b}	$57.73 \pm 3.27^{b,A}$
- Epicatechin Liposomal	5	5.0	1000	-	73.99 ± 1.27^{a}	$-20.00 \pm 1.27^{b,d}$	48.28 ± 1.03^{b}	$49.16 \pm 2.25^{c,A}$

Cocoa extract-loaded liposome**	5	5.0	1000	-	84.3 ± 0.07^{c}	-22.85 ± 2.54^{d}	-	-
- Theobromine							0.05 ± 0.04^{a}	8.44 ± 0.74^{a,A}
- Caffeine							0.07 ± 0.06^{a}	31.49 ± 2.68^{b,A}
- Catechin							48.99 ± 0.27^{b}	30.58 ± 3.3^{b,A}
- Epicatechin							61.10 ± 0.06^{c}	27.51 ± 1.86^{b,A}
Formulation-in-aqueous-system								
Free cocoa extract**	-	-	1000	-	-	-	-	-
- Theobromine								26.60 ± 1.21^{a,B}
- Caffeine								83.50 ± 10.80^{b,B}
- Catechin								13.07 ± 4.46^{a,B}
- Epicatechin								12.59 ± 3.56^{a,B}
Free compounds	-	-	-	-	-	-	-	-
- Theobromine			1000					79.37 ± 4.73^{a,B}
- Caffeine			1000					75.09 ± 5.96^{a,B}
- Catechin			1000					29.38 ± 2.51^{b,B}
- Epicatechin			1000					22.55 ± 3.63^{b,B}

*Liposomes produced by optimal condition for both microfluidization and sonication method (more details in methodology section). ** The concentration of alkaloids, catechins and procyanidins (up to hexamer) were calculated from the HPLC analysis. Then, the percentage of each compound was determined, and thus the molarity contribution of each compound. The sum of all compounds were used as the total molarity of the total alkaloids, catechins and procyanidins. Means within a column in the same box that share the same letter are not significantly different by Tukey ($p > 0.05$). Means within a column in different box with different capital letters (A, B) indicate significant differences ($p<0.05$) between the bioaccessibility for the different bioactive compounds (compounds-loaded liposomes vs non-encapsulated compounds and cocoa extract-loaded liposomes vs free cocoa extract).

Table 2. ABTS (µmol Trolox/ µmol sample) and DPPH (scavenging activity, %) Antioxidant Assays of Tested Compounds Before, and After the Gastric and Duodenal Phases of *In Vitro* Gastrointestinal Conditions.

ABTS Assay						
	Free compounds			**Compounds-loaded liposomes**		
Compound	**Initial**	**Gastric**	**Duodenal**	**Initial**	**Gastric**	**Duodenal**
Theobromine	< LOQ	< LOQ	0.44 ± 0.00^{a,A}	0.05 ± 0.21^{a}	1.08 ± 0.01^{a}	0.91 ± 0.18^{a,B}
Caffeine	< LOQ	< LOQ	0.40 ± 0.00^{a,A}	0.05 ± 1.00^{a}	1.12 ± 0.01^{a}	0.94 ± 0.18^{a,B}
Catechin	0.90 ± 0.03^{c,A}	1.76 ± 0.08^{b,A}	7.06 ± 0.13^{b,A}	1.41 ± 0.03^{b,B}	4.78 ± 0.04^{b,c,B}	6.01 ± 0.15^{b,B}
Epicatechin	0.96 ± 0.02^{c,A}	2.27 ± 0.05^{b,A}	5.79 ± 0.13^{c,A}	1.48 ± 0.02^{b,B}	4.73 ± 0.05^{b,B}	6.29 ± 0.25^{b,A}
Cocoa extract	0.62 ± 0.03^{d,A}	3.70 ± 0.05^{c,A}	8.85 ± 0.07^{d,A}	1.66 ± 0.03^{b,B}	4.97 ± 0.02^{c,B}	13.41 ± 0.40^{c,B}
DPPH Assay						
Unloaded Liposome				14.88 ± 1.46^{a}	16.27 ± 1.45^{a}	32.95 ± 1.43^{a}
Theobromine	15.77 ± 0.73^{a,A}	15.77 ± 2.16^{a,A}	16.65 ± 1.63^{a,A}	16.94 ± 0.95^{a,b,A}	20.74 ± 0.44^{a,B}	39.18 ± 1.97^{b,B}
Caffeine	16.12 ± 1.18^{a,A}	16.68 ± 0.88^{a,A}	17.18 ± 0.83^{a,A}	17.41 ± 1.43^{b,A}	20.59 ± 0.94^{a,B}	41.18 ± 0.97^{b,B}
Catechin	> 100^{b}	66.01 ± 0.92^{b,A}	92.49 ± 0.35^{b,A}	> 100^{c}	43.95 ± 1.68^{b,B}	91.19 ± 0.54^{c,A}
Epicatechin	> 100^{b}	75.19 ± 0.77^{b,c,A}	95.24 ± 1.39^{b,A}	> 100^{c}	46.42 ± 1.86^{b,B}	92.96 ± 3.54^{c,A}
Cocoa extract	> 100^{b}	80.25 ± 10.63^{c,A}	81.54 ± 1.76^{c,A}	> 100^{c}	93.08 ± 3.04^{c,A}	> 100^{d,B}

Means within a column (comparison between same digestion phases for the different bioactive compounds) with different letter are significantly different by Tukey ($p < 0.05$). Means within a column in different box with different capital letters (A, B) indicate significant differences ($p<0.05$) between same digestion stage for the same bioactive compounds. LOQ = 0.20 µM Trolox.

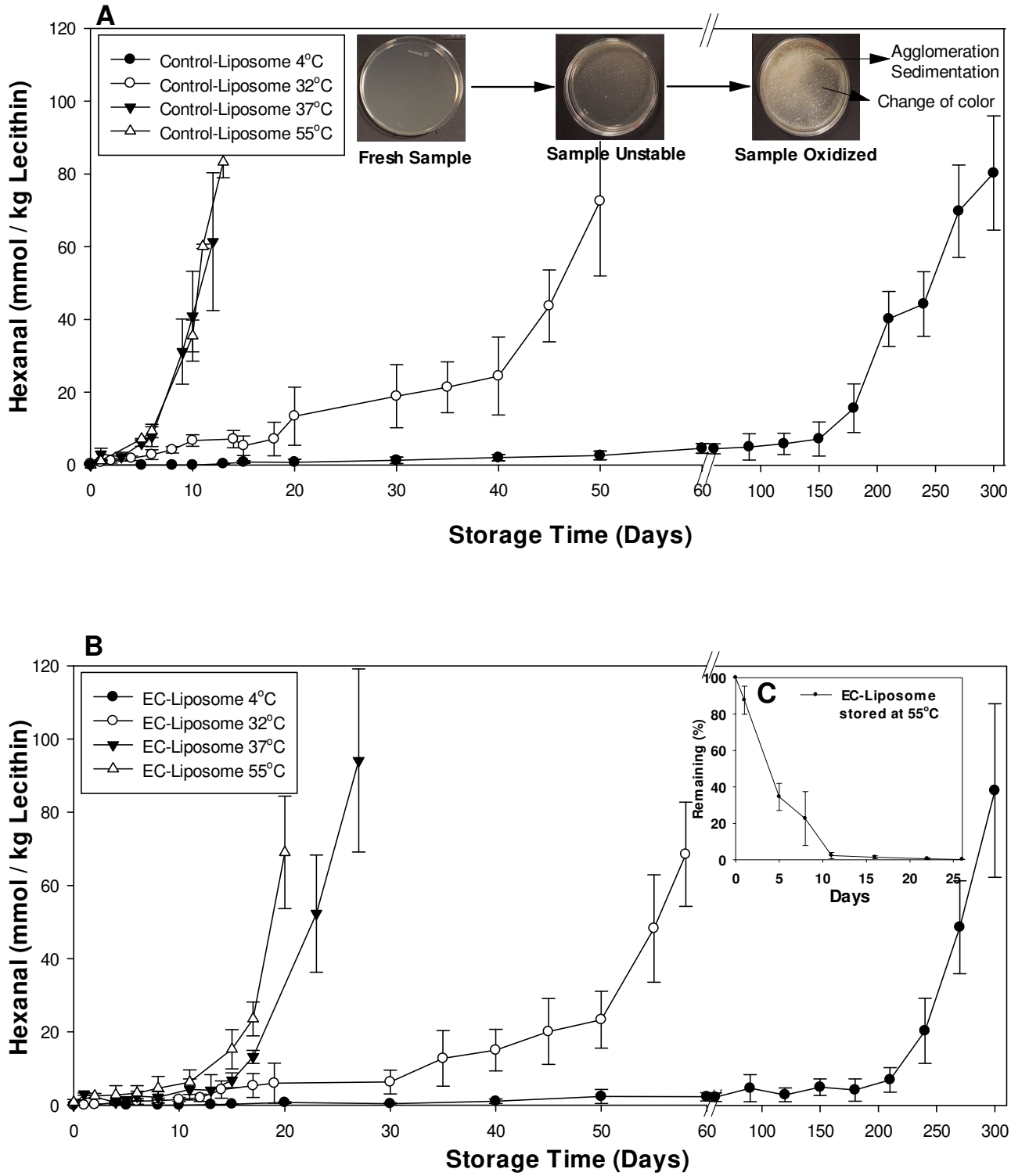
A
Control-Liposome 4°C
Control-Liposome 32°C
Control-Liposome 37°C
Control-Liposome 55°C
Fresh Sample
Sample Unstable
Sample Oxidized
Agglomeration
Sedimentation
Change of color
Hexanal (mmol / kg Lecithin)
Storage Time (Days)
B
EC-Liposome 4°C
EC-Liposome 32°C
EC-Liposome 37°C
EC-Liposome 55°C
C
EC-Liposome stored at 55°C
Remaining (%)
Days
Hexanal (mmol / kg Lecithin)
Storage Time (Days)

Figure 1.

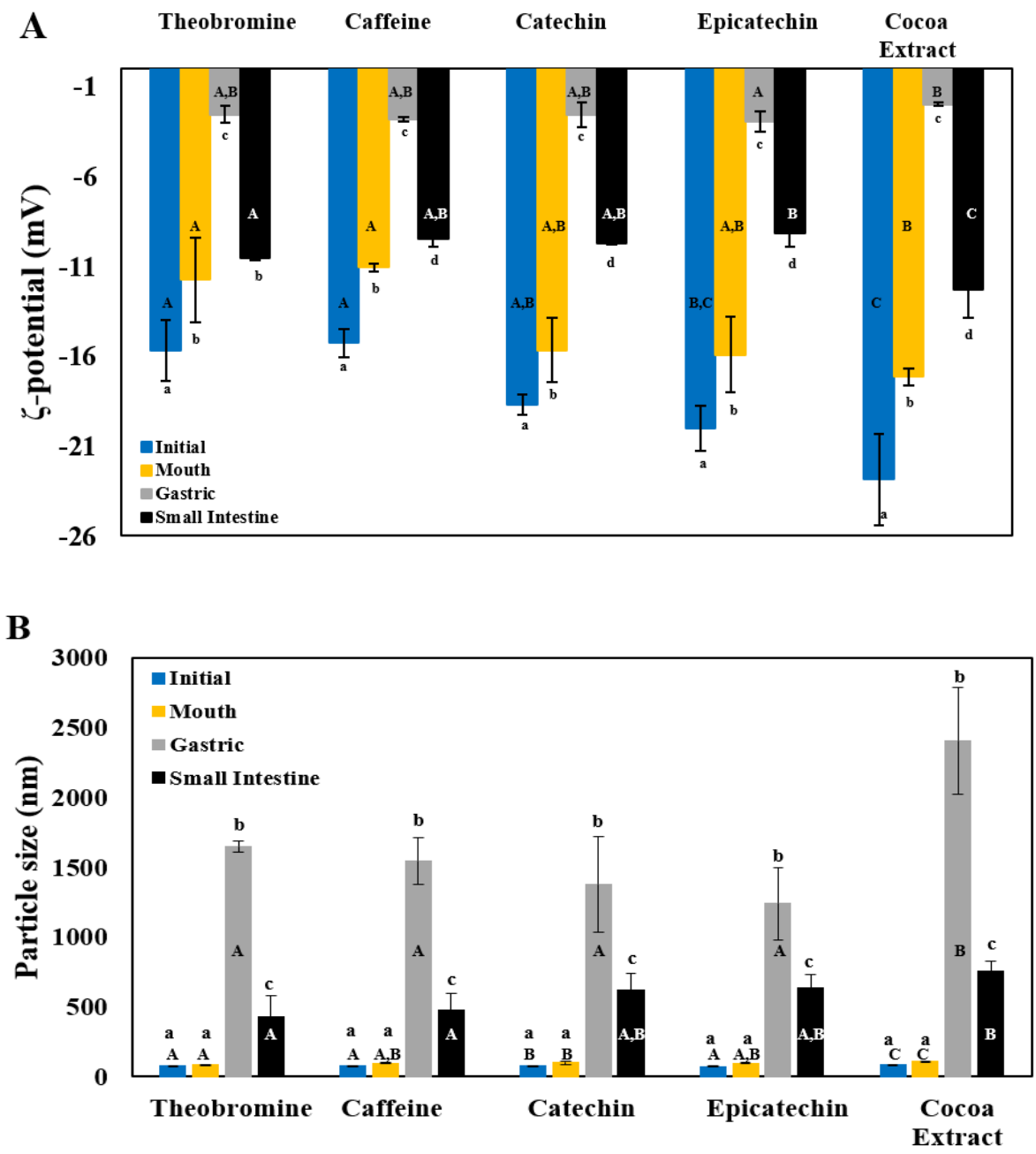
A
Theobromine
Caffeine
Catechin
Epicatechin
Cocoa Extract
ζ-potential (mV)
-1
-6
-11
-16
-21
-26
Initial
Mouth
Gastric
Small Intestine
B
Particle size (nm)
3000
2500
2000
1500
1000
500
0
Initial
Mouth
Gastric
Small Intestine
Theobromine
Caffeine
Catechin
Epicatechin
Cocoa Extract

Figure 2.

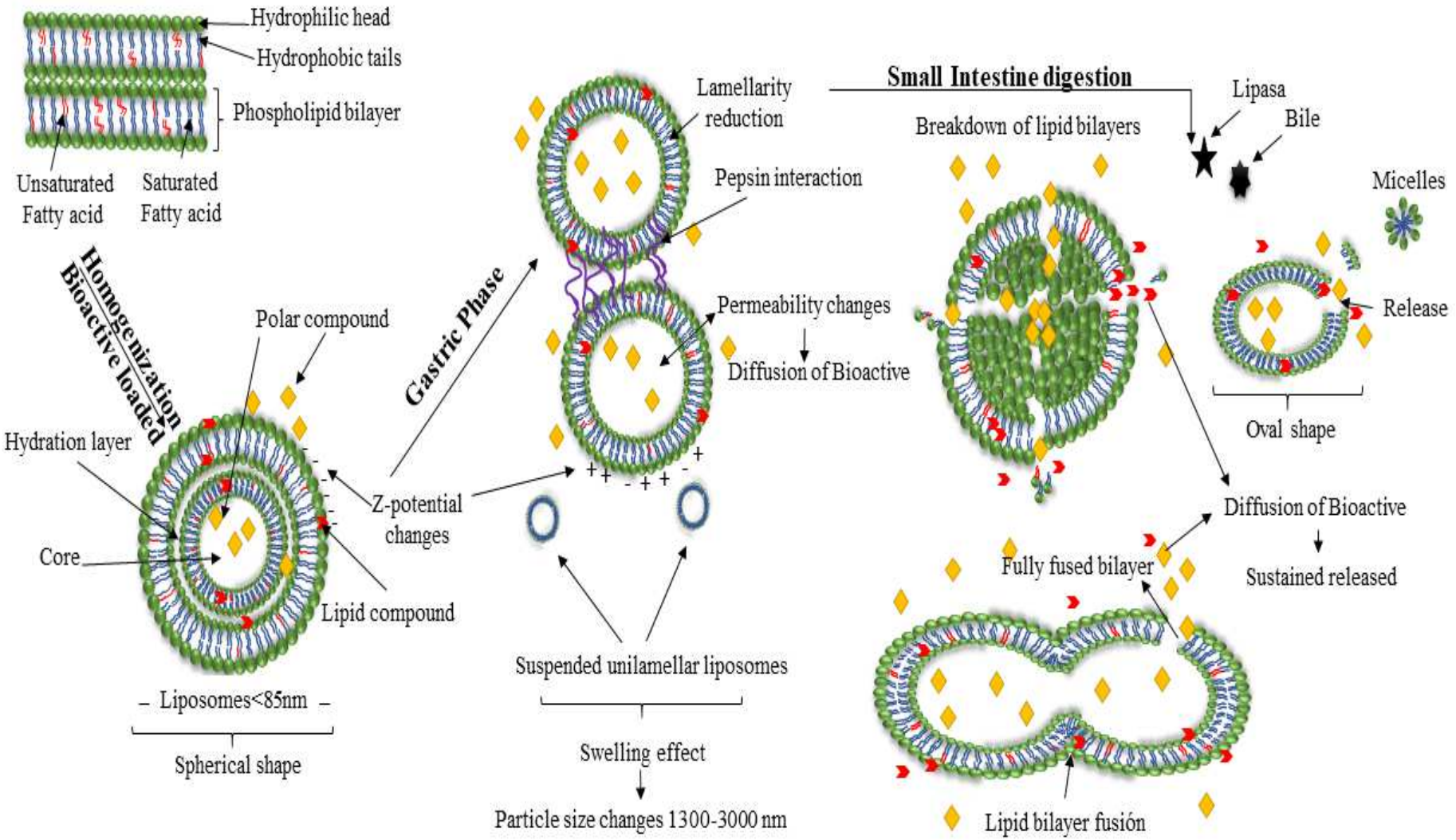
Hydrophilic head
Hydrophobic tails
Phospholipid bilayer
Unsaturated Fatty acid
Saturated Fatty acid
Homogenization
Bioactive loaded
Polar compound
Hydration layer
Core
Lipid compound
Z-potential changes
Liposomes<85nm
Spherical shape
Gastric Phase
Lamellarity reduction
Pepsin interaction
Permeability changes
Diffusion of Bioactive
Suspended unilamellar liposomes
Swelling effect
Particle size changes 1300-3000 nm
Small Intestine digestion
Lipasa
Bile
Breakdown of lipid bilayers
Micelles
Release
Oval shape
Diffusion of Bioactive
Sustained released
Fully fused bilayer
Lipid bilayer fusión

Figure 3.

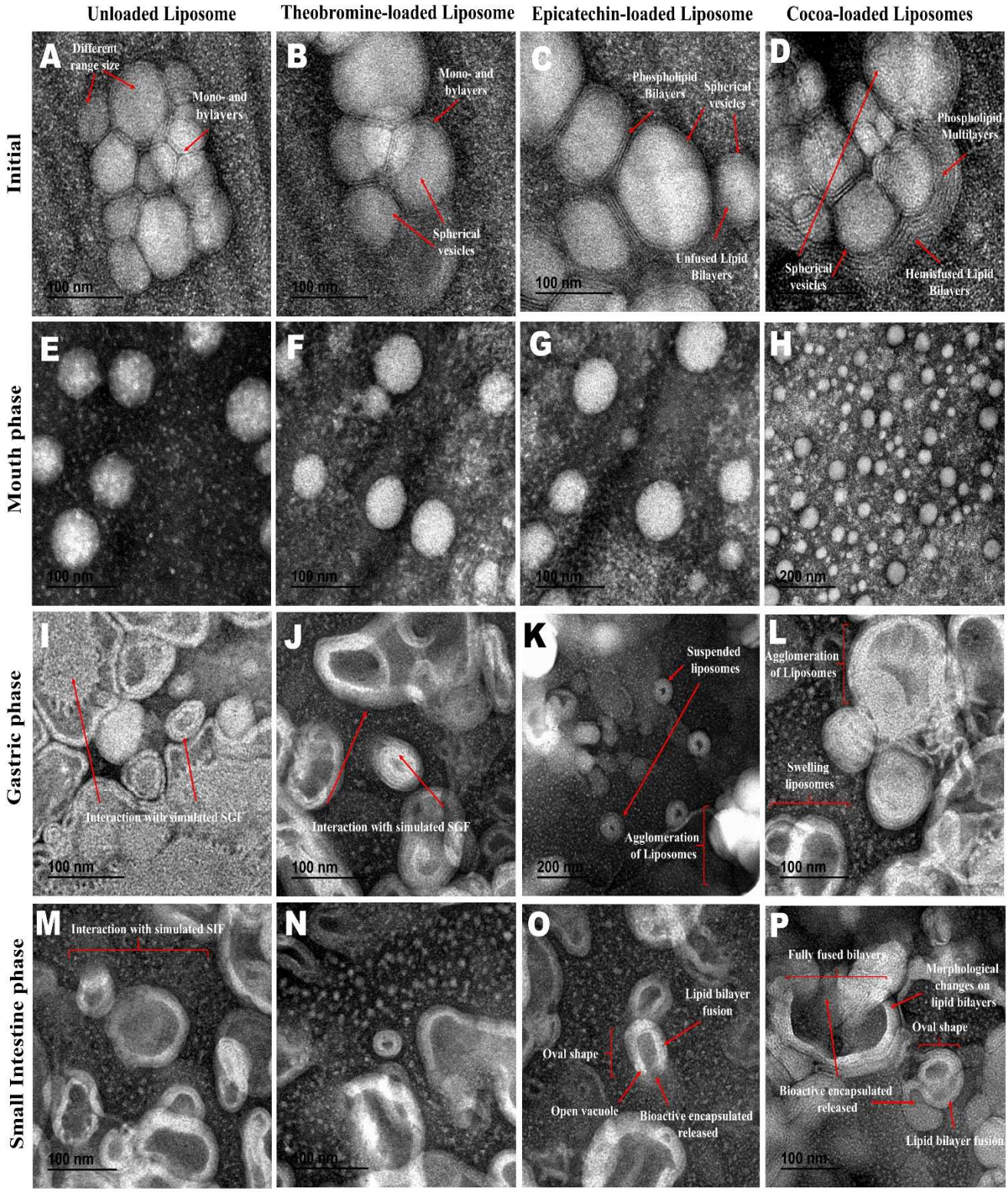
Unloaded Liposome
Theobromine-loaded Liposome
Epicatechin-loaded Liposome
Cocoa-loaded Liposomes
Initial
Mouth phase
Gastric phase
Small Intestine phase
A
Different range size
Mono- and bylayers
B
Mono- and bylayers
Spherical vesicles
C
Phospholipid Bilayers
Spherical vesicles
Unfused Lipid Bilayers
D
Phospholipid Multilayers
Spherical vesicles
Hemisfused Lipid Bilayers
E
F
G
H
I
Interaction with simulated SGF
J
Interaction with simulated SGF
K
Suspended liposomes
Agglomeration of Liposomes
L
Agglomeration of Liposomes
Swelling liposomes
M
Interaction with simulated SIF
N
O
Lipid bilayer fusion
Oval shape
Open vacuole
Bioactive encapsulated released
P
Fully fused bilayers
Morphological changes on lipid bilayers
Oval shape
Bioactive encapsulated released
Lipid bilayer fusion
100 nm
200 nm

Figure 4.

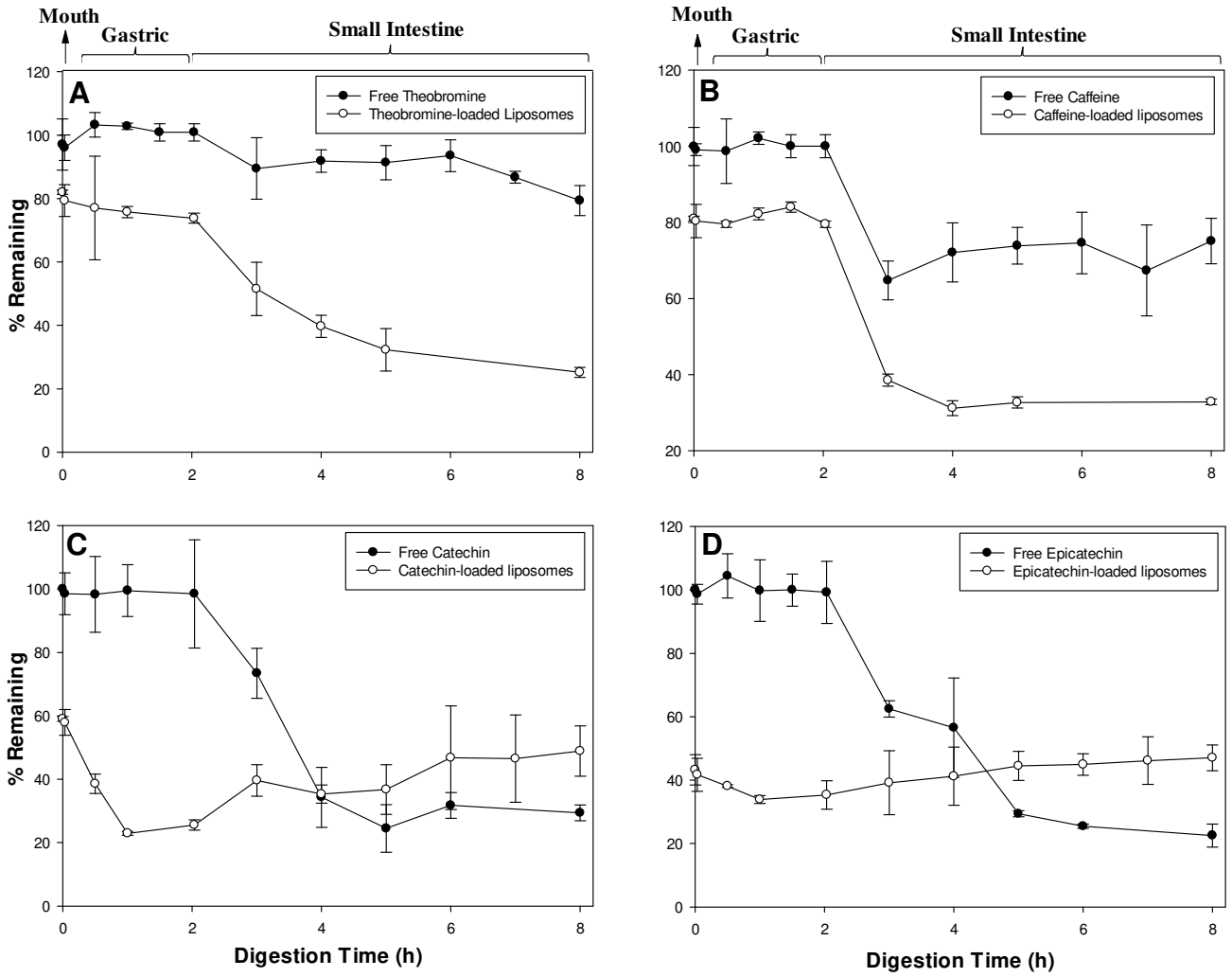
Mouth
Gastric
Small Intestine
A
Free Theobromine
Theobromine-loaded Liposomes
% Remaining
B
Free Caffeine
Caffeine-loaded liposomes
C
Free Catechin
Catechin-loaded liposomes
% Remaining
D
Free Epicatechin
Epicatechin-loaded liposomes
Digestion Time (h)
Digestion Time (h)

Figure 5.

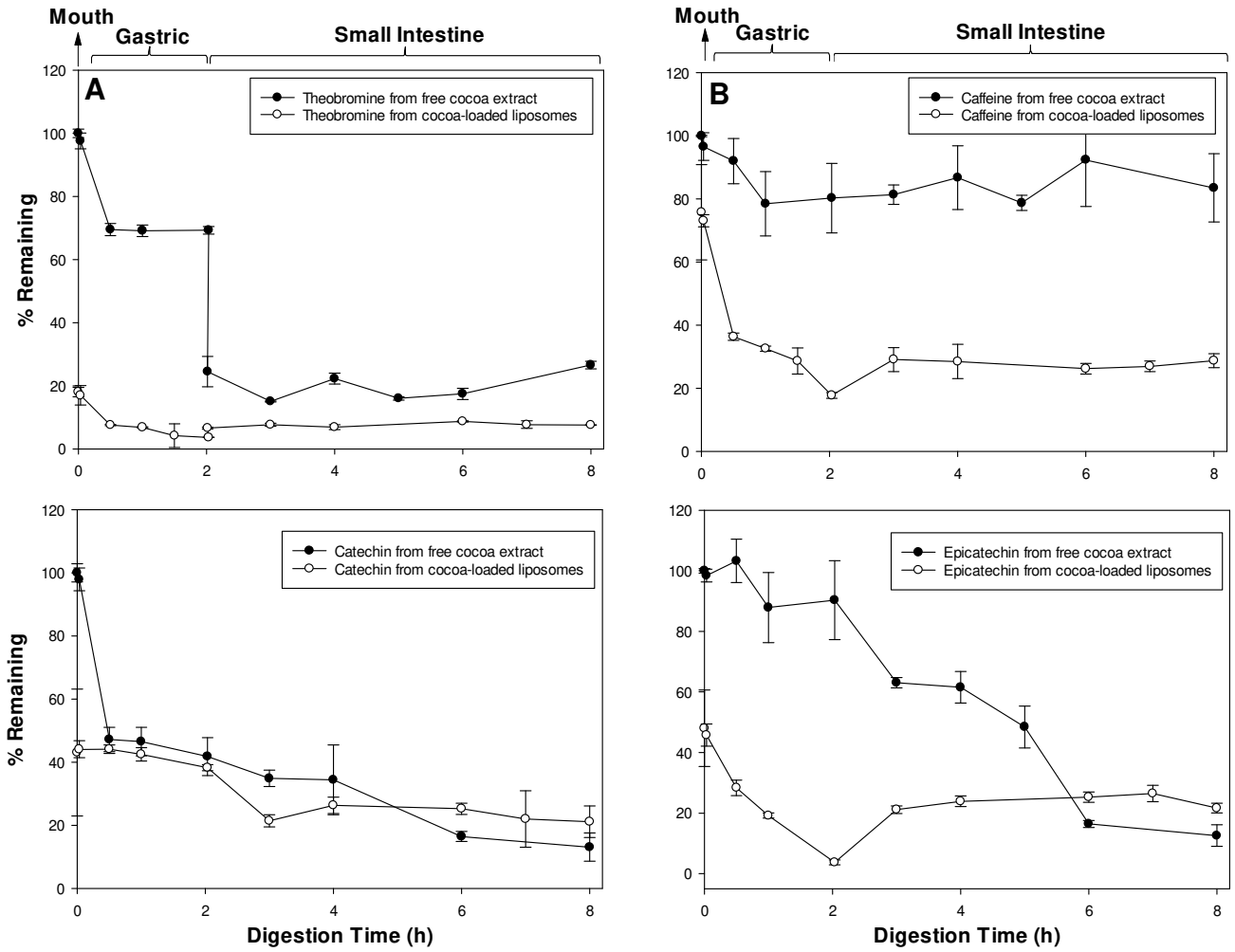
Mouth
Gastric
Small Intestine
A
Theobromine from free cocoa extract
Theobromine from cocoa-loaded liposomes
% Remaining
B
Caffeine from free cocoa extract
Caffeine from cocoa-loaded liposomes
Catechin from free cocoa extract
Catechin from cocoa-loaded liposomes
Epicatechin from free cocoa extract
Epicatechin from cocoa-loaded liposomes
Digestion Time (h)

Figure 6.

Table of Contents Graphic (TOC)